Received: 12 December 2017 | Revised: 18 January 2018 | Accepted: 18 January 2018

DOI: 10.1002/cne.24398

RESEARCH ARTICLE

WILEY The Journal of Comparative Neurology

Representation of the stomatopod's retinal midband in the optic lobes: Putative neural substrates for integrating chromatic, achromatic and polarization information

Hanne Halkinrud Thoen[1] | Marcel E. Sayre[2] | Justin Marshall[1] | Nicholas James Strausfeld[2]

[1]Sensory Neurobiology Group, Queensland Brain Institute, University of Queensland, Brisbane, Australia

[2]Department of Neuroscience, School of Mind, Brain and Behavior, University of Arizona, Tucson, Arizona

Correspondence
Hanne Halkinrud Thoen, Queensland Brain Institute, University of Queensland, QBI Building 79, St Lucia, St Lucia, Brisbane, QLD 4072, Australia.
Email: h.thoen@uq.edu.au

Funding information
Asian Office of Aerospace Research and Development, Grant/Award Number: FA2386-13-1-4134; U.S Air Force Research Laboratory, Grant/Award Number: FA8651-13-1-0001, FA8651-17-P-0121; Center for Insect Science, University of Arizona; Australian Research Council, Grant/Award Number: FL140100197; Lizard Island Research Foundation

Abstract

Stomatopods have an elaborate visual system served by a retina that is unique to this class of pancrustaceans. Its upper and lower eye hemispheres encode luminance and linear polarization while an equatorial band of photoreceptors termed the midband detects color, circularly polarized light and linear polarization in the ultraviolet. In common with many malacostracan crustaceans, stomatopods have stalked eyes, but they can move these independently within three degrees of rotational freedom. Both eyes separately use saccadic and scanning movements but they can also move in a coordinated fashion to track selected targets or maintain a forward eyestalk posture during swimming. Visual information is initially processed in the first two optic neuropils, the lamina and the medulla, where the eye's midband is represented by enlarged regions within each neuropil that contain populations of neurons, the axons of which are segregated from the neuropil regions subtending the hemispheres. Neuronal channels representing the midband extend from the medulla to the lobula where populations of putative inhibitory glutamic acid decarboxylase-positive neurons and tyrosine hydroxylase-positive neurons intrinsic to the lobula have specific associations with the midband. Here we investigate the organization of the midband representation in the medulla and the lobula in the context of their overall architecture. We discuss the implications of observed arrangements, in which midband inputs to the lobula send out collaterals that extend across the retinotopic mosaic pertaining to the hemispheres. This organization suggests an integrative design that diverges from the eumalacostracan ground pattern and, for the stomatopod, enables color and polarization information to be integrated with luminance information that presumably encodes shape and motion.

KEYWORDS

Bodian, color, Golgi impregnation, immunocytology, optic lobes, polarization, Stomatopoda, vision, RRID:AB_528479, RRID:AB_1157911, RRID:AB_572268, RRID:AB_ 477019, RRID: AB_2632953, RRID:AB_572263

1 | INTRODUCTION

1.1 | Stomatopod vision and neural architecture

Stomatopods have the most elaborate visual system of any pancrustacean and indeed perhaps any invertebrate. Their retinas are equipped with a specialized midband zone of ommatidia providing 12 photoreceptor channels sampling colors ranging from the ultraviolet to the far red, in addition to several types of achromatic receptors, some of which detect linear and circular polarized light (Marshall, 1988; Cronin & Marshall, 1989; Cronin, Marshall, & Caldwell, 1993; Cronin, Marshall, & Land, 1994; Marshall & Oberwinkler, 1999; Marshall, Cronin, & Kleinlogel, 2007; Chiou et al., 2008; Templin, How, Roberts, Chiou, & Marshall, 2017, Thoen, Chiou, & Marshall, 2017a). The retinal midband consists of 6 rows of ommatidia, four of which mediate the detection

J_ID: Customer A_ID: CNE24398 Cadmus Art: CNE24398 Ed. Ref. No.: JCN-17-0275.R1 Date: 3-February-18 Stage: Page: 2

of chromatic information (Figure 1a). Ommatidia in adjacent rows 5 and 6 are each equipped with seven rhabdomeres that detect circularly polarized light in the mid-spectrum around 500 nm, and distal R8 photoreceptor cells that both detect linear polarized light in the ultraviolet (UV) and serve as an optical 1/4-wave retarder for the underlying seven photoreceptors (Chiou et al., 2008, Roberts, Chiou, Marshall, & Cronin, 2009). The many thousands of ommatidia comprising the hemispheres of the eye are equipped with luminance and linearly polarization sensitive receptors receptive in four different directions of electrical vector (e-vector) sensitivity.

Previous descriptions have documented the midband's representation in the lamina by enlarged neurons, and in the medulla by an outswelling where those neurons terminate (Kleinlogel, Marshall, Horwood, & Land, 2003; Kleinlogel & Marshall, 2005; Thoen, Strausfeld, & Marshall, 2017b). In the lamina, photoreceptor terminals from the retina's midband are larger than those from the hemispheres, as are monopolar cells and other interneurons associated with the midband (Figure 1a, b). Thus, optic cartridges (each representing one visual sampling unit or ommatidium) that are supplied by the midband are at least twice the diameter of optic cartridges subtending the hemispheral ommatidia where the general organization of neurons appears to be similar to morphological types described from other eumalacostracan crustaceans (Thoen et al., 2017b). The midband is likewise represented by an enlarged hernia-like outswelling across the width of the medulla at its midline (Figure 1c, d).

Signals from the retina are processed through three nested optic neuropils (Figure 1d), before information is segregated to higher order processing centers in the lateral protocerebrum within the eye stalk, and the central brain. Monopolar cells relaying information from the midband photoreceptors project their axons across the first optic chiasm to reach the outswelling of the medulla, here termed the medulla's midband protuberance, MMP. Except at the MMP, the medulla is composed of a regular arrangement of columns (Figure 1d, e), each representing a visual sampling unit or ommatidium. Clusters of relay neurons (transmedullary cells) comprise each column and their grouped terminals map the medulla's retinotopy into various depths of the lobula. The affinity of MMP transmedullary cells to antibodies raised against tyrosine hydroxylase, and the correspondence of these to expanded arrangements of dendrites within the MMP (Figure 2a–d) further amplify the special status of this pathway. Throughout the medulla, except at the MMP, transmedullary neurons are intersected by planar arrangements of local interneurons and other networks provided by centrifugal pathways and lateral processes of efferent neurons. However, antibodies against synapsin (Figure 1c) demonstrate that axons of neurons relating to the MMP are not contacted by those layers, as the MMP axons pass through them to the lobula. The exception is in the medulla's deepest level (Figure 2a) where collaterals from MMP transmedullary cells do spread out laterally suggesting that the MMP relays could interact with columns flanking the MMP pathway (Figure 2a, d, c), an organization that is reiterated at levels in the lobula.

Here we focus on the organization of neurons originating in the MMP supplying the lobula. We address the question how color information might be integrated within this visual system. Neuroanatomical evidence suggests that color integration does not occur across the medulla in a manner that is known for other invertebrates with color vision, such as the bee or fruit fly (Paulk, Phillips-Portillo, Dacks, Fellous, & Gronenberg, 2008; Lebhart & Desplan, 2017; Lin et al., 2016), in which color channels are distributed across the entire eye (Rister & Desplan, 2011, Lin et al., 2016; Lebhart & Desplan, 2017). Rather, we show that chromatic relays from the stompatopod's retinal midband appear to be separate from those representing the hemispheres. The organization in stomatopods seems to be radically different from that in Hexapoda. It is also distinct from other Eucrustacea where evidence suggests that mono- or dichromacy is the norm (Marshall, Kent, & Cronin, 1999). However, because MMP relays have collateral arrangements in the inner medulla we cannot discount the potential for color information integrating with the rest of the eye already at that level.

In insects with color vision, the chromatic pathway is distributed across the lobula's retinotopic organization whereas in stomatopods color channels are restricted to the retinal midband. We hypothesize that if color is integrated with achromatic channels from the hemispheres then the neuroanatomical organization of channels from the midband will suggest one or more physiological interpretations. Here we show that midband channels do provide systems of collaterals that would allow combinatorial integration across the entire relayed visual field. We also describe neurons with wide dendritic fields across many retinotopic units that are reminiscent of neurons described from insects that detect visual flow for balance during forward motion.

2 | MATERIALS AND METHODS

2.1 | Immunocytochemistry

Antibodies used for this study are listed in Table 1. Neuropils were labeled with monoclonal antisynapsin (3C11, "SYNORF"), previously used on malacostracans (Sullivan & Beltz, 2004), that recognizes at least four synapsin isoforms (70, 74, 80, and 143 kDa, Klagges et al., 1996). Serotonergic processes were resolved using an antibody against serotonin (5HT) previously used to label neurons in several crustacean species including stomatopods (Derby, Fortier, Harrison, & Cate 2003; Wolff, Thoen, Marshall, Sayre, & Strausfeld, 2017) A monoclonal tyrosine hydroxylase (TH) antibody raised in rats was used to selectively resolve midband neurons, together with an antibody against the synthesizing enzyme glutamic acid decarboxylase (GAD). As shown previously, both identify neurons immunoreactive to antibodies against dopamine and GABA, respectively (Wolff et al., 2017). Neuropil processes were revealed by an α-tubulin monoclonal antibody while F-actin was resolved using phalloidin.

Animals were anesthetized on ice, decapitated and the nervous tissue dissected out in cold (4°C) fixative (4% paraformaldehyde with 10% sucrose in phosphate-buffered saline, pH 7.4 (PBS, Sigma, St Louis, MO). Nervous tissue labeled for synapsin was fixed overnight at 4°C. Tissue used for other antibodies, except anti-TH, was fixed at 18°C using a microwave oven (two cycles of 2 min with power and 2 min under vacuum) before being left overnight at 4°C in fresh fixative. After fixation, tissue was washed for 3 × 10 min in PBS and embedded using

ID: jwaa3b2server Time: 18:22 I Path: //chenas03.cadmus.com/Cenpro/ApplicationFiles/Journals/Wiley/CNE#/Vol00000/180008/Comp/APPFile/JW-CNE#180008

J_ID: Customer A_ID: **CNE24398** Cadmus Art: **CNE24398** Ed. Ref. No.: **JCN-17-0275.R1** Date: **3-February-18** Stage: Page: **3**

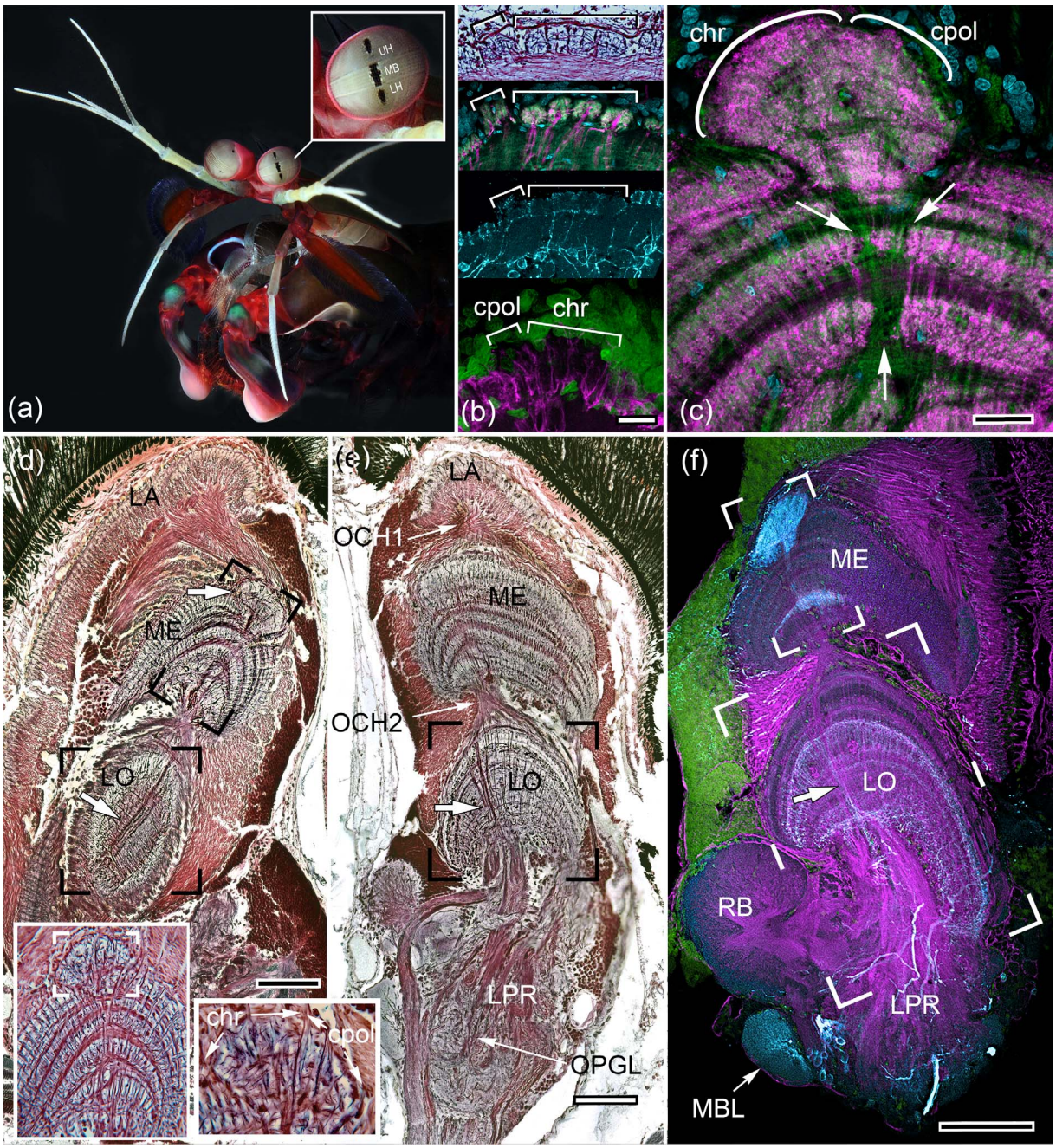

COLOR IN ONLINE AND PRINT

FIGURE 1 Representation of the retinal midband through the stomatopod visual system. (a). The head of the stomatopod *Gonodactylus smithii* showing in the inset the division of the eye into an upper and lower hemisphere (UH, LH) separated by the horizontally oriented retinal midband (MB). (b). Representation of the midband in the lamina. Upper image: Bodian-stained lamina showing enlarged optic cartridges. Second image: synapsin/actin immunostaining showing monopolar cell neurons (magenta) of the four largest optic cartridges receiving inputs (green) from the four chromatic midband channels (chr) adjacent to a pair of smaller cartridges receiving inputs from the circular polarized light/UV channels (cpol). Enlargement of midband cartridges are reflected by the organization of TH- and GAD-positive centrifugal terminals (cyan: third image, magenta, lower image). (c). Synapsin-actin immunostaining of the medulla showing its midband protuberance (MMP) flanked by columns of the hemispheres. Arrows indicate the synapsin-free trajectory from the protuberance through the medulla. The chr and cpol domains in the MMP are reversed due to cross-over of axons in the first optic chiasma. (d, e, f) Organization of optic lobe neuropils in the vertical (d) and horizontal (e, f) planes to show the lamina (LA) connected by the first optic chiasma (OCH1) to the medulla (ME), and medulla connected by the second chiasma (OCH2) to the lobula. Arrows in d indicate the MMP in the medulla and its representation in the lobula, here sectioned tangential to its surface. Boxed areas refer to the enlargements of the MMP in the two insets, lower left. Boxed area of the lobula refers to the enlarged depiction of the midband in Figure 8a. Outputs from the lobula extend to optic glomeruli (OPGL) in the lateral protocerebrum (LPR). (f). Overview of the optic lobes and the enlarged reniform body (RB) that flanks its ventrolateral edge, distal to one of the mushroom body lobes (MBL). Neuropils have been labeled with α-tubulin (magenta), cell bodies with syto 13 (green) and projections from the MMP in the medulla (boxed area) and its representation through the lobula (arrowed) (LO) are revealed by their TH-immunoreactivity (cyan). Scale bars: (b, c) 25 μm; (d–f) 200 μm

ID: **jwaa3b2server** Time: 18:22 I Path: //chenas03.cadmus.com/Cenpro/ApplicationFiles/Journals/Wiley/CNE#/Vol00000/180008/Comp/APPFile/JW-CNE#180008

J_ID: Customer A_ID: CNE24398 Cadmus Art: CNE24398 Ed. Ref. No.: JCN-17-0275.R1 Date: 3-February-18 Stage: Page: 4

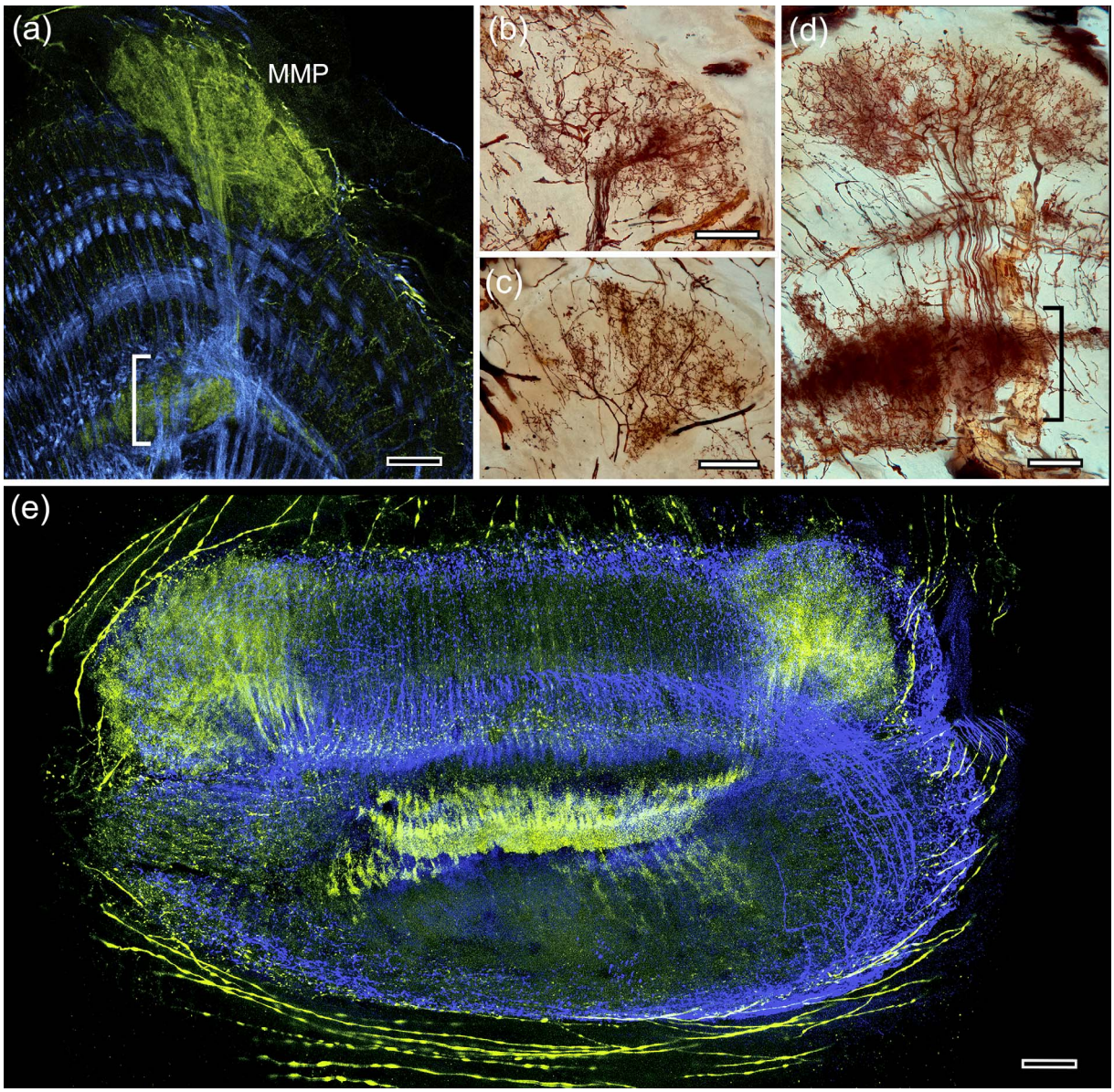

COLOR IN ONLINE AND PRINT

FIGURE 2 The medulla midband protuberance (MMP). (a) Anti-TH immunostaining (yellow) specifically resolves the representation of the retinal midband in the MMP and through the medulla's inner layers (bracketed). Reactivity against α-tubulin is shown in blue. (b–d). Golgi-impregnated spiny (b) and varicose (c, d) arborizations of MMP neurons that extend through the medulla to branch in its inner layers (bracketed in a, d). (e). Section taken tangential to the surface of the medulla showing TH-immunoreactive transmedullary neurons from the MMP (yellow) and the linear representation of the retinal midband by its inner immunoreactivity processes. Serotonergic processes are shown in blue. Scale bars: (a, e) 50 μm, (b–d) 25 μm

albumin gelatin. Sections were cut at 60–150 μm on a Leica vibratome, washed for 6 × 20 min in 0.1 M PBS with 0.5% Triton X-100 (X-100, Sigma Aldrich) (PBS-TX) and preincubated for 1 hr in 0.1 M PBS with 0.2% Triton X-100 and 5% normal goat serum (NGS, 50–062Z, Life-Technologies, Carlsbad, CA). Sections were incubated with antibodies at concentrations given in Table 1 in 0.1 M PBS with 0.5% Triton X-100 and 5% NGS overnight on a shaker at room temperature.

After incubation, sections were rinsed for 5 × 10 min in 0.1 M PBS before being treated as follows: 1,000 μL aliquots of PBS-TX were placed in tubes with 0.25% secondary Cy2, Cy3 or Cy5 conjugated IgGs (Jackson ImmunoResearch, West Grove, PA) and centrifuged at 13,000 rpm for 15 min at 4°C. From this solution the top 900 μL was added to the well containing the sections. Wells were left on a slow shaker at room temperature overnight, before being washed 6 × 30 min in 0.1 M PBS. Some sections were additionally incubated in the fluorescent nuclear stain Syto-13 (Life Technologies, Grand Island, NY) at a concentration of 1:2,000 for 1 hr. Completed sections were mounted on slides, coverslipped under an admixture of 25% polyvinyl alcohol, 25% glycerol and 50% PBS.

Tissue treated with antibodies against tyrosine hydroxylase was fixed in 4% paraformaldehyde in 0.1 M PBS with 10% sucrose at 4°C for 30 min. Tissue was then soaked for 2 hr in PBS containing 1% Triton X-100 before being transferred to 1% PBS-TX and 5% normal donkey serum (Jackson ImmunoResearch Labs, Cat. no. 017-000-121). Tissue remained

J_ID: Customer A_ID: CNE24398 Cadmus Art: CNE24398 Ed. Ref. No.: JCN-17-0275.R1 Date: 3-February-18 Stage: Page: 5

TABLE 1 Antibodies

Antibody	Immunogen	Supplier and RRID	Host	Concentration
Synapsin "SYNORF 1"	A glutathione S–transferase-fusion protein including a portion of a Drosophila synapsin homolog	DSHB, # 3C11, RRID: AB_528479	Mouse (monoclonal)	1:50
Alpha-tubulin	Alpha-tubulin from a mixture of *Tetrahymena thermophila* and *Tetrahymena pyriformis*	DSHB, #12G10, RRID: AB_1157911	Mouse (monoclonal)	1:100
Tyrosine hydroxylase	Purified from PC12 cells and recognizes the 34 kDa catalytic core of TH.	IHW #22941, RRID: AB_572268	Rats (monoclonal)	1:250
GAD	Synthetic peptide corresponding to the C-terminal region of human GAD 67	SA, G5163, RRID:AB_ 477019	Rabbit, (polyclonal)	1:1,000
F-actin	Phalloidin conjugated to Alexa Fluor 546	TFS, A-22283. RRID: AB_2632953		1:40
Serotonin	Serotonin coupled to bovine serum (BSA) with paraformaldehyde	IHW, 20080, RRID: AB_572263	Rabbit (polyclonal)	1:500

DSHB, Developmental Studies Hybridoma Bank; IHW, ImmunoStar, Hudson, WI; SA, Sigma-Aldrich; TFS, Thermo Fisher Scientific.

in this solution for 2 hr before adding the primary antibody. The TH primary antibody was then added, and left for 48 hr at room temperature on a gentle shake before being washed several times over 3 hr in 0.5% PBS-TX. Following the washing step, the tissue was incubated in a secondary antibody conjugated to Cy5 (Jackson ImmunoResearch, West Grove, PA, Cat. no. 715-175-150). After at least 24 hr, tissue was washed several times in PBS-TX, and then sectioned, immunolabeled with a additional primary antibody and secondary antibody, incubated with the Syto-13 nuclear stain, and mounted as described above.

2.2 | Tracer application

Visualization of axons from the lobula to destinations in the lateral protocerebrum were carried out using a method described by Ehmer and Gronenberg (2002). Crystals of dextran labeled with Texas red (MW 3000) were placed on a glass slide resting on ice. Condensation on the slide then liquified the dextran into a paste-like consistency, which could be collected as a small droplet on the tip of a pulled glass microelectrode before being allowed to air dry. Animals were anesthetised on ice before a small opening was cut in eyestalk cuticle providing access to the optic lobes. The microelectrode was inserted into an area of interest and left in place for about 20 sec. Next, the microelectrode was removed and the area closed using the removed patch of cuticle. Animals were then returned to seawater and maintained for 4–6 hr to allow the dye to spread. Then, the specimen was killed, its nervous tissue dissected out and fixed in 4% paraformaldehyde in 0.1 M PBS at 4°C overnight. The next day tissue was washed in buffer, embedded in 5% LMP agarose, sectioned at 150 μm and mounted on slides using 80% glycerol in 0.1 M PBS.

2.3 | Golgi impregnations

Stochastic silver impregnations were performed using a variation of the mixed Colonnier-rapid technique (Li & Strausfeld, 1997) as described in Wolff et al. (2017).

2.4 | Bodian reduced silver stain

Reduced silver staining was carried out using Bodian's (1936) original method.

2.5 | Image aquisition and image processing

Tissue treated for immunocytology or tracer dyes were imaged by confocal microscopy using either a Zeiss LSM 710 inverted point-scanning confocal or a Zeiss Pascal confocal microscope equipped with oil immersion objectives. Maximum projection images were made using the z-project plugin in the open source software Fiji (Schindelin et al., 2012) and brightness, contrast and color balance was adjusted using Adobe Photoshop CC. Light microscopy images were obtained with a Leitz Orthoplan microscope or a Zeiss Axio Imager microscope allowing automated step focusing and image stitching. Complex images were reconstructed manually or using the software Helicon Focus (Helicon Soft, Kharkov, Ukraine; RRID: SCR_014462).

3 | RESULTS

3.1 | General overview of the lobula complex

Here we report the first description of the stomatopod lobula, also noting its relationship to discrete proximal neuropils of the lateral protocerebrum and the distal neuropil, the medulla. Departing from convention, throughout the Results we provide interpretive remarks where these assist the descriptive narrative. Further aspects of medulla neuroarchitecture will be described in separate works currently in preparation.

Historically viewed as a single neuropil termed the medulla terminalis, the lateral protocerebrum has recently been recognized as consisting of many small well-defined centers that are involved in multisensory processing and integration, including higher visual processing. This overall organization corresponds to the insect lateral

J_ID: Customer A_ID: CNE24398 Cadmus Art: CNE24398 Ed. Ref. No.: JCN-17-0275.R1 Date: 3-February-18 Stage: Page: 6

protocerebrum (Wolff & Strausfeld, 2016; Wolff et al., 2017, fig. 1 supplement 2).

The stomatopod lobula is a deep kidney-shaped neuropil lying proximal to the medulla (Figure 1d–f) from which it receives retinotopic inputs via the second optic chiasma. The lobula is also accompanied by a diminutive satellite neuropil lying alongside it that may or may not correspond to the lobula plate as described mainly in insects (see Section 2.1).

The lobula is composed of columns intersected by stratified arrangements of synaptic networks. This stratification is extensive, defining at least 13 discrete layers comprising an organization that distinguishes the stomatopod lobula from those of other pancrustacans. Each lobula column, which represents one visual sampling point, is composed of a defined set of neurons each having a characteristic morphology. As in insects, the axons of each morphological type converge beneath the lobula to target a defined neuropil called an optic glomerulus situated in the lateral protocerebrum (Strausfeld, Sinakevitch, & Okamura, 2007). In Malacostraca, lobula columns are spaced like the columns in the medulla, each corresponding to a visual sampling unit, the photoreceptors of one ommatidium sharing the same optical axis, making the whole system a "fine-grained" retinotopy until the deepest level in the lobula (Strausfeld, 1998; Sztarker, Strausfeld, & Tomsic, 2005). This is an important difference from insects, where the spacing of lobula columns coarsens the representation of the peripheral retinotopic mosaic: in insects one lobula column represents 6–9 visual sampling points. Dendritic fields from a column overlap those of neighboring columns, so that neurons of the column receive inputs from at least one axial and six surrounding visual sampling units. The only known exception thus far is in Odonata (dragonflies, darters) where lobula columns at some levels appear to be as densely spaced as columns in the medulla (unpublished observations).

The following description outlines the lobula's overall morphology to provide the structural context of this neuropil into which midband relays extend.

3.2 | Organization of the stomatopod lobula

Although being the homologue of the lobula in other pancrustaceans, the stomatopod lobula has a highly divergent morphology. It is stunningly elaborate. Apart from its specialized representation of the retinal midband, the density and retinotopic spacing of its columnar efferent neurons and the multiplicity of synaptic strata that intersect their passage through the lobula is even more intricate than the most elaborate insect or crustacean medullas, neuropils that generally show greater stratification and neuronal morphologies than the lobulas. Here, we will restrict the present description to the stomatopod lobula's overall morphology. Detailed portrayals of individual neuronal morphologies and central projections will be described in subsequent studies.

The lobula's distal surface lacks any midband swelling comparable to that of the medulla. Other than being punctuated by incoming axons from the medulla, the surface is uniformly smooth. However, the midband is clearly distinguished through the lobula by the passage of axons of its specialized neurons, which are shown by reduced silver stains (Figure 3a), as well as anti-synapsin (Figure 3b), anti-tyrosine hydroxylase, and anti-GAD immunolabeling (Figure 3c, d). F3

The overall neuroarchitecture of the lobula representing the hemispheres is demonstrated by reduced silver stains that show an isomorphic arrangement of retinotopic columns intersected by stratified arrangements of synaptic networks. Sections cut vertically and horizontally, normal to the lobula's outer surface show at least 13 distinct layers, each identified by its stratified organization, which at some levels further divide a layer into thinner synaptic strata (Figure 4a, b). F4 These planar arrangements include the most delicate of arborizations with diameters less that 1 μm in diameter to substantial processes comparable to the largest tangential neurons identified in insects. Stratified networks are composed of local interneuron processes (Figures 4c, 6f), F6 the dendrites of wide-field tangential cells (Figures 4d, 6a–e) and the lateral processes—both postsynaptic dendritic and presynaptic collateral extensions—belonging to densely packed columnar neurons (Figure 5). These efferent neurons extend through the lobula and send their F5 axons into the lateral protocerebrum where they target optic glomeruli, which are volumes of synaptic neuropils comparable to glomeruli of insect optic lobes (Mu, Ito, Bacon, & Strausfeld, 2012). Tangential cells provide systems of extensive branches that extend uninterrupted throughout a stratum so as to subtend large areas of the hemispheric regions. Examples of large diameter tangentials are shown in Figure 6b. However, there are just as many smaller tangential neurons at corresponding and other levels (Figure 6c) as well as systems of tiered tangential processes that serve widely separate strata linked by columnar branches (Figure 6e). Terminals occurring at numerous levels in the lobula (Figure 4c) demonstrate that inputs from the medulla segregate to various levels in its outer strata, as occurs in the lobulas of insects.

Because the Golgi method stochastically impregnates neurons, without additional criteria it is not possible to confidently claim that any neuron with a specific morphology is nothing other than an example of a certain type that occurs in every retinotopic column. Mass impregnations, as in Figure 5, demonstrate such arrangements, but single neurons like those having inverted Y-shaped collaterals in Figure 4c, d, provide no such information unless they can be confirmed by other methods as belonging to the lobula's midband. The following provides anatomical criteria which, however, suggest that these neurons are indeed components of the midband.

3.3 | Midband representation in the lobula

Information from the retina's midband is relayed by the lamina's midband monopolar cells to the MMP where they terminate in a reversed retinotopic order of 4 chromatic + 2 circular polarization visual sampling units (Figure 1b–d). The terminals of these monopolar cells extend into a system of profuse dendrites that occupy the volume of the outswelling (Figures 1c, 2a–d). Labeling with anti-synapsin demonstrates the MMP is denoted by its abundance of synaptic sites, more than the numbers at corresponding levels of columns that subtend the hemispheres (Figure 1c). Such synaptic density suggests that signals from the lamina's midband are amplified by postsynaptic neurons in MMP. In the medulla, beneath the level of

J_ID: Customer A_ID: CNE24398 Cadmus Art: CNE24398 Ed. Ref. No.: JCN-17-0275.R1 Date: 3-February-18 Stage: Page: 7

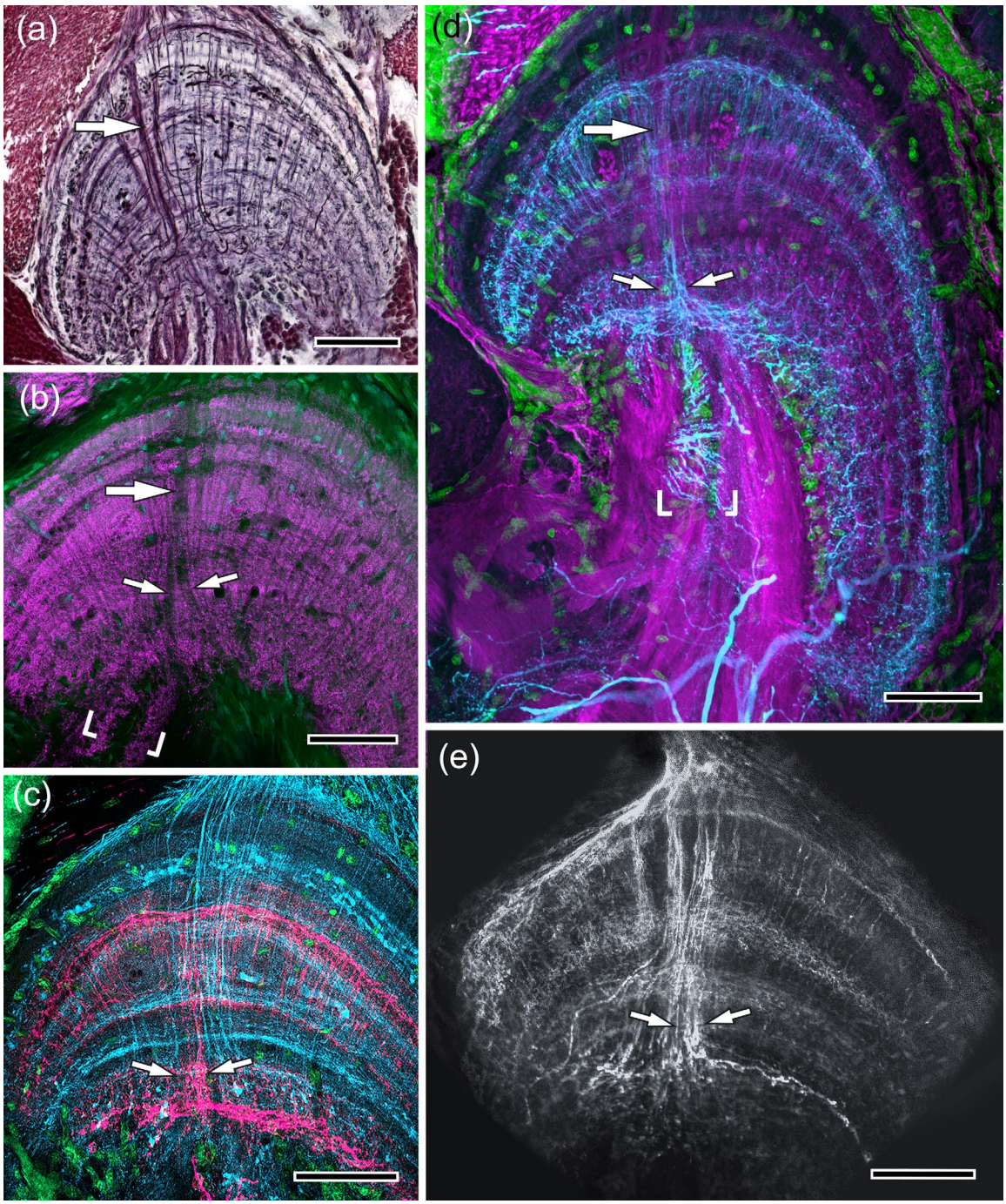

COLOR IN ONLINE AND PRINT

FIGURE 3 The midband trajectory through the lobula. (a–c). Bodian reduced silver (a), synapsin/actin (pink/green, respectively) (b) and TH (magenta in c, cyan in d) and GAD (cyan in c) immunostaining demonstrate the passage of MMP transmedullary cell axons through the lobula (arrows). Across the horizontal extent of the lobula, this passage constitutes a curtain of axons that separates the lobula's upper and lower regions. Typically, the passage of axons in the curtain splits as an inverted Y in the deep layers of the neuropil. This profile reflects the passage of collaterals that extend from midband axons as shown in panel e. Anti-synapsin reveals a tongue of neuropil (bracketed) contiguous with the midband trajectory. The tongue is also revealed by TH immunostaining (bracketed in d). (e). Fluorescent tracers applied in vivo to the medulla label neurons extending into the lobula and in so doing resolve terminals specific to the retinal midband representation. Here several terminals of MMP transmedullary neurons are shown in the deep lobula layers with branched trajectories matching those resolved by immunocytology. Scale bars: 50 μm

its MMP, the midband is clearly represented as a strip of axons through the medulla (Figure 1d). This strip cuts horizontally across the medulla's width and in so doing interrupts the medulla's stratified organization and thereby clearly distinguishes the hemispheric representation of the medulla (Figure 1d). Axons from MMP neurons project directly through the medulla in this narrow zone that unlike the rest of the medulla's depth is almost devoid of stratified networks (Figure 1c).

J_ID: Customer A_ID: CNE24398 Cadmus Art: CNE24398 Ed. Ref. No.: JCN-17-0275.R1 Date: 3-February-18 Stage: Page: 8

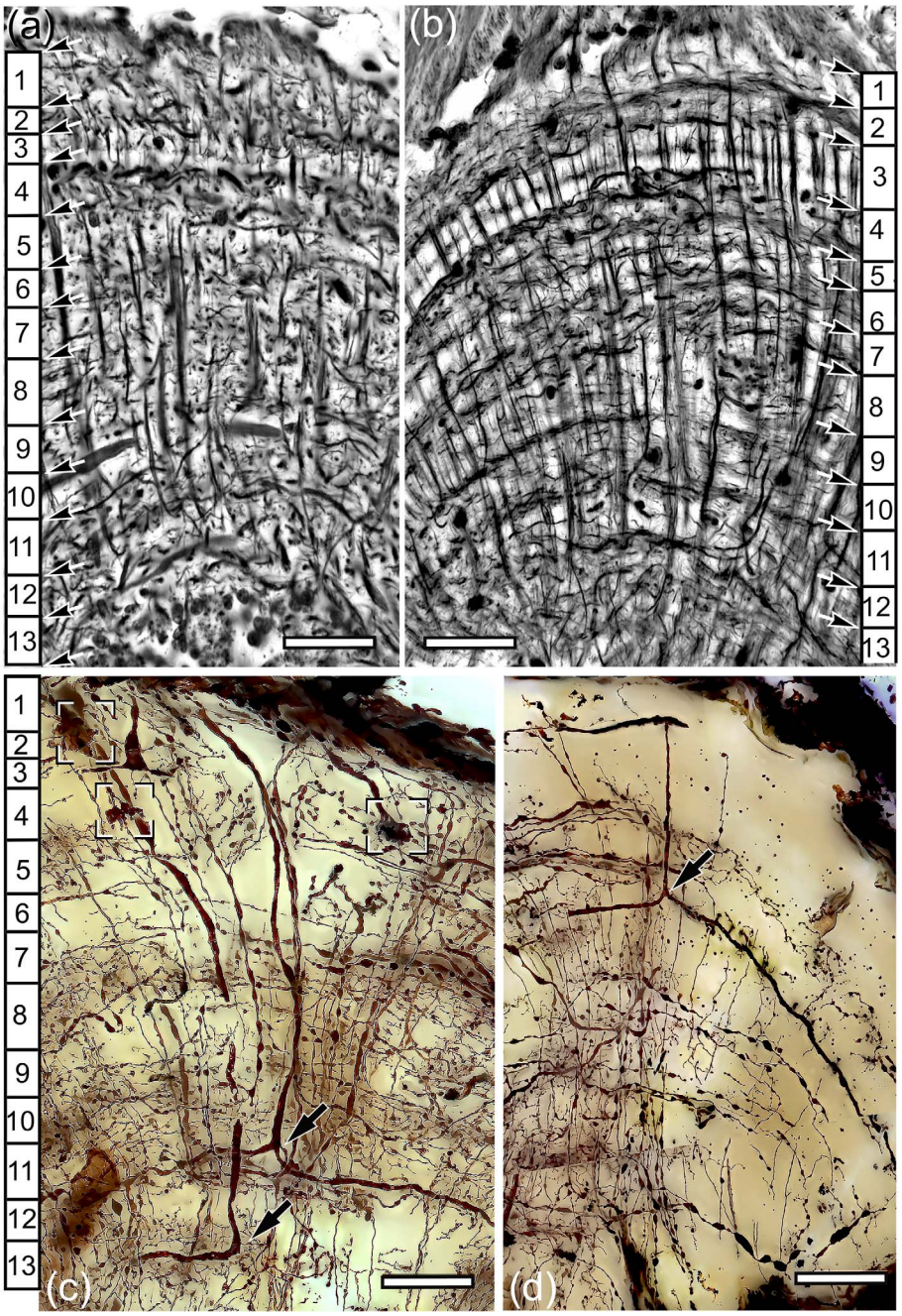

COLOR IN ONLINE AND PRINT

FIGURE 4 Lobula layers and afferents. The columnar organization of the lobula appears different in sections cut along the lobula's vertical (a) and horizontal (b) axes. Bodian reduced silver best resolves discrete layers that relate to the processes of Golgi and tracer-filled neurons. Thirteen discrete layers are resolved by reduced silver, many of which are further subdivided by smaller strata, such as layers 3, 4 in (b). (c). Golgi impregnation resolves terminals from the medulla (boxed) limited to single retinotopic columns. These end at many levels of which only three are shown here. Prominent inverted Y-shaped terminals end in layers 10–13, and more distally in layers 5/6 (panel c). The former correspond to tracer-filled terminals shown in Figure 3e. Also notable are the many layers of slender processes and their branches extending tangentially within strata, indicating systems of local interneurons. Scale bars: 25 μm

The R8 cells from both the midband and the hemispheres also terminate in the medulla as would be expected of a malacostracan. In stomatopods there is some evidence for differences in the en-passant lamina synapses between chromatic and achromatic ommatidia (Kleinlogel & Marshall 2005).

Midband axons extend from the medulla's inner face into the second optic chiasma, reversing their anteroposterior order again before entering the lobula. The axons then project deep into the lobula again interrupting the strata of tangentially disposed processes (Figures 1d, e, 7a, b). Tracer dye injections into the medulla resolve neuron morphologies that are constrained to, and extend processes from, the midband projection (Figure 7a–f). Notably, midband neurons ending in the lobula do so within its inner layers and are most densely arranged at levels corresponding to layers 10–13 (Figure 7a, c–f; see Figure 4a, b). The F7

J_ID: Customer A_ID: CNE24398 Cadmus Art: CNE24398 Ed. Ref. No.: JCN-17-0275.R1 Date: 3-February-18 Stage: Page: 9

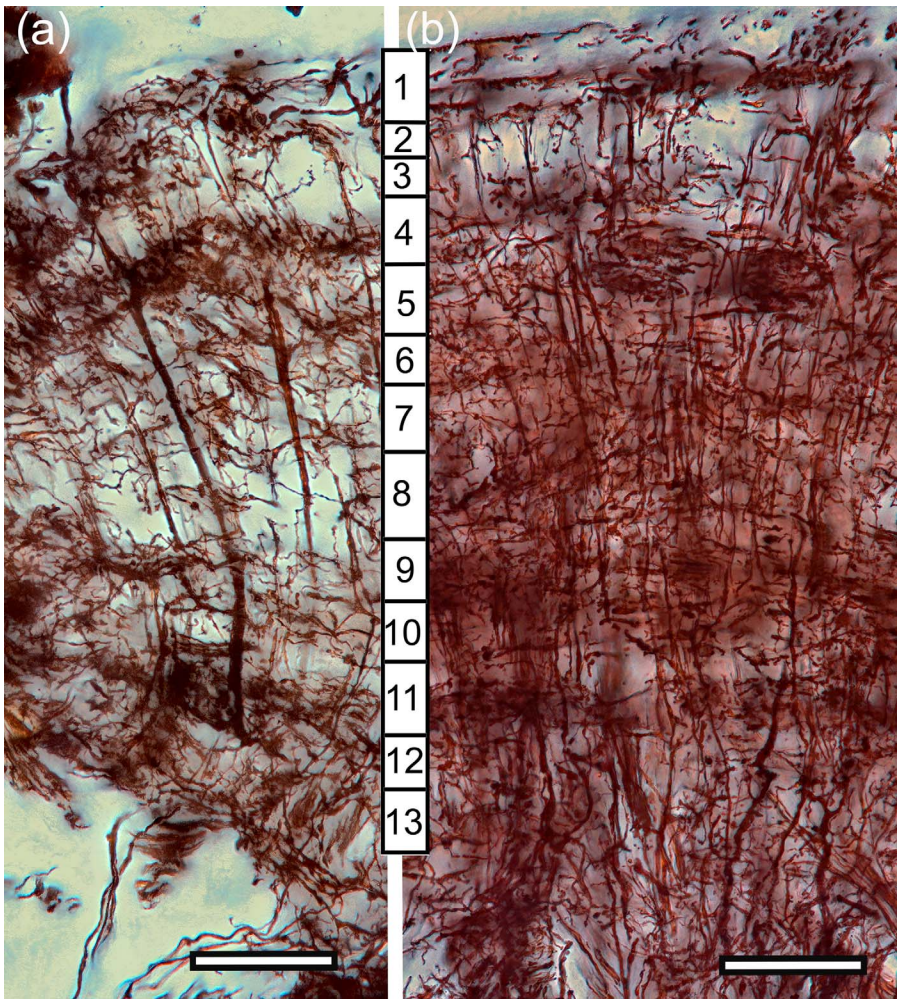

COLOR IN ONLINE AND PRINT

FIGURE 5 Columnar organization of efferent neurons. The lobula is retinotopically organized into columns, each of which comprises a set of numerous efferent (output) neurons. These examples (a, b) demonstrate Golgi-impregnated efferents with prominent axons, from which arise distal dendrites and deeper collaterals (panel a). (b). Mass Golgi-impregnations provide one view of the complexity in the lobula, here provided by hundreds of efferent neurons each characterized by a slender axon less than 4 μm in diameter. Despite their density, the occurrence of dendrites and collaterals though the lobula correspond to specific reduced-silver stained layers. Scale bars: 50 μm

midband projection does not, however, terminate exclusively in the lobula. Rather, some of its neurons project deeper into a tongue of neuropil extending from beneath the lobula's inner face. First identified from anti-synapsin labeling (Figure 3b), and also denoted by anti-tyrosine hydroxylase (Figure 3d), this neuropil is denoted by a tangle of large dendrites belonging to efferent neurons extending into the lateral protocerebrum (Figure 7b).

Midband terminals in the lobula have a characteristic morphology within the region's inner levels (Figure 8a). Sections cut tangential to the lobula's surface demonstrate two adjacent rows of axons extending into these layers, one row corresponding to the midband chromatic receptors and the other assumed to correspond to the midband c-pol receptors. Each of these rows gives rise to systems of lateral collaterals, those from the chromatic row being more substantial than those from the c-pol row (Figure 8b, c), with both resolved by mass Golgi impregnations (Figure 8f, g). Together, all the midband axons in the lobula establish a curtain-like cascade that divides the neuropil into an upper and lower half. Terminals of midband columnar neurons impose a broad, thick, carpet-like layer of collaterals that extend vertically from each side of the midband so as to intercept columns representing the hemispheres. We will return to this arrangement of terminal collaterals in Section 2.1 when asking why interactions between midband relays and the hemispheral relays appear to occur so deep in the system.

There is also evidence that, unexpectedly, the representation of the midband does not end in the lobula, or in the tongue of neuropil extending beneath it. Reduced silver preparations show that flanking each side of the midband tongue is a row of regularly spaced axons that extend centrally into the lateral protocerebrum (Figure 8d, e). To ascertain their central destination will require targeted tracer experiments.

One spectacular organization at this level is revealed by immunolabeling with antibodies raised against tyrosine hydroxylase. At least three TH-positive systems relate to the lobula' midband. One is derived from wide-field neurons that provide processes at the level of lobula layer 6, parallel to a system of large diameter GAD-positive tangential neurons in layer 4 (Figure 9a, b). Anti-GAD immunostaining also

J_ID: Customer A_ID: CNE24398 Cadmus Art: CNE24398 Ed. Ref. No.: JCN-17-0275.R1 Date: 3-February-18 Stage: Page: 10

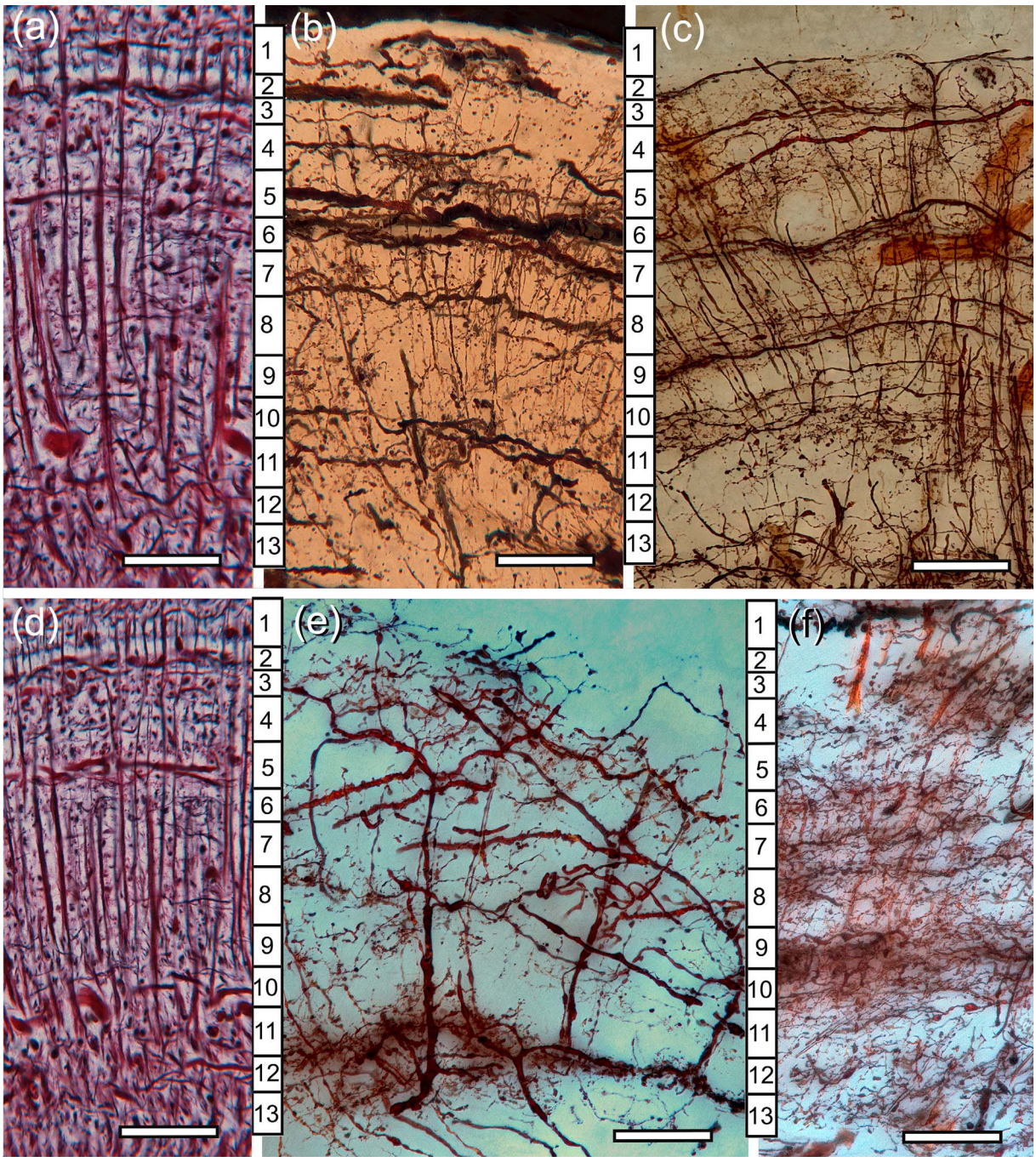

COLOR IN ONLINE AND PRINT

FIGURE 6 Tangential organization in the lobula. Layers and their strata in Bodian stained lobulas (a, d) correspond to the layered disposition of Golgi-impregnated tangential dendrites and terminals. These occur throughout the lobula, with diameters ranging from 15 μm, such as the large elements in layers 2, 5, and 6 (panel b) to less than 3 μm (smallest elements in panel c). Note that some tangentials "switch" layers, such as the element in layer 5 to the left in panel (c), extending obliquely to level 3 toward the right. (e). Bistratified tangential neurons with branches at layer 3, 4, and deep at layers 11, 12 give rise to axons that leave the inner face of the lobula. (f). Layered arrangements of local interneuron processes. These impart a further level of elaboration to the stomatopod lobula, defining it as very different from the corresponding neuropil of the insect optic lobe. Scale bars: 50 μm

resolves GAD-positive columnar cells specific to the lobula midband, the terminals of which correspond to neurons dye-filled from the medulla (compare Figures 9a and 7a). Two further systems of TH-positive local interneurons derive from a clone of cell bodies lying beneath and to the side of the lobula (Figure 9c). These give rise to a cascade-like arrangement of stratified and columnar processes extending between lobula layers 6 and 8 (Figure 9a) and a second system within layer 11 and 13. The deepest processes of this second system adopt the same laterally extending morphology as do the collaterals extending from terminals of midband columnar neurons (Figure 9a, d). Thus, tyrosine hydroxylase defines the midband both in the medulla and in the lobula.

J_ID: Customer A_ID: CNE24398 Cadmus Art: CNE24398 Ed. Ref. No.: JCN-17-0275.R1 Date: 3-February-18 Stage: Page: 11

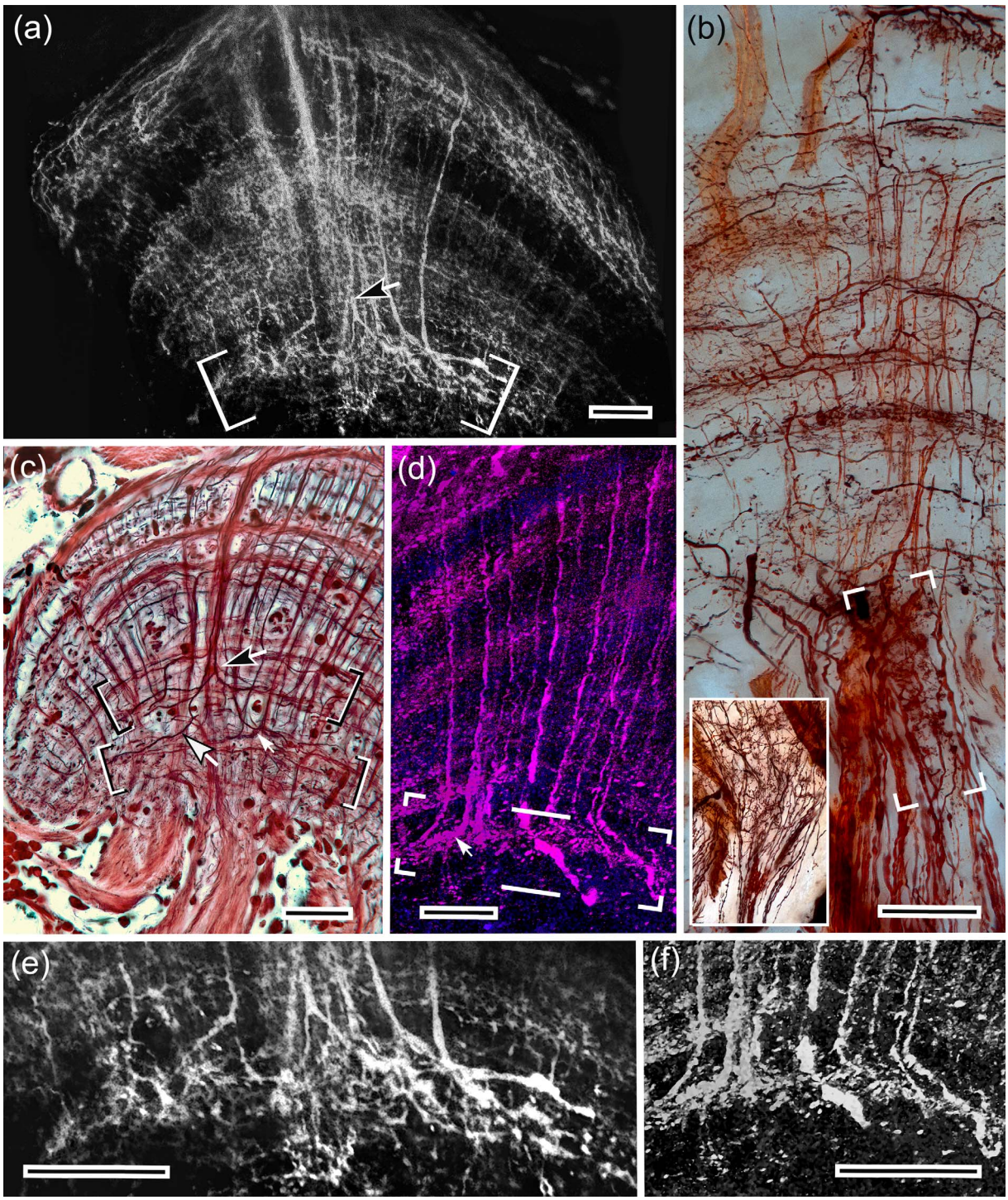

COLOR IN ONLINE AND PRINT

FIGURE 7 Identity of midband terminals in the lobula. (a). Tracer fluorescent dyes applied to the medulla resolve terminals in layers 11–12 in the lobula that represent the retinal midband. Terminals show their characteristic inverted Y bifurcation (arrow). (b). Golgi impregnated lobula showing tangential layering intersecting the passage of small intrinsic fibers associated with the midband "curtain" that extend into the midband tongue (boxed area and inset lower left). (c). Bodian stained lobula resolving two major levels of bifurcating terminals from MMP transmedullary cells, the branches of which extend across flanking retinotopic columns. The outer branches (filled arrow) extend laterally within layers 8–9. The inner branches (open arrow) extend within layers 11, 12. The small white arrow indicates a small bifurcating terminal corresponding to dye-filled neurons in the adjacent panel. (d). Section taken parallel to the long axis of the midband "curtain" showing tracer-filled MMP transmedullary cells with narrow-field bifurcating terminals in layer 11, 12. (e, f). Details of MMP transmedullary cell terminals in layers 11, 12. Scale bars: 50 μm

J_ID: Customer A_ID: CNE24398 Cadmus Art: CNE24398 Ed. Ref. No.: JCN-17-0275.R1 Date: 3-February-18 Stage: Page: 12

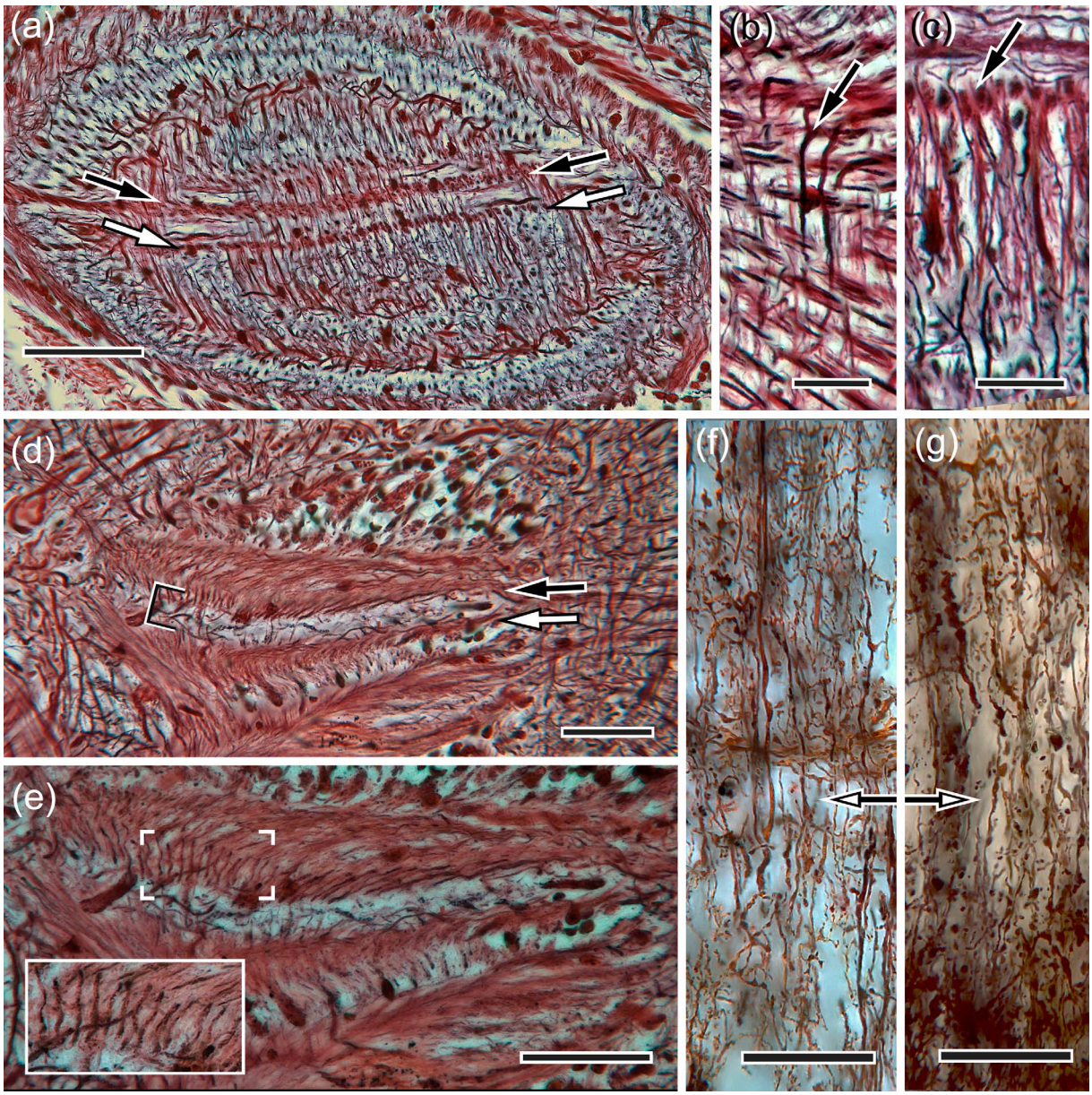

COLOR IN ONLINE AND PRINT

FIGURE 8 Representation of the midband in the lobula. (a) A section across a Bodian-stained lobula, at about layers 8–10, oriented such that the representation of the horizontal midband extends across the panel. Filled and open arrows indicate two rows midband axons cut transversely, the upper row corresponding to the chromatic channels and the lower row to the c-pol channels. Collaterals extend from these rows vertically to intersect retinotopic columns representing the upper and lower hemispheres. (b, c) Detail of collaterals from the upper and lower rows indicated in panel (a). (d) Section cut parallel to the inner face of the lobula, beneath layer 13, showing the midband tongue neuropil flanked by the cross sections of two rows of axons extending out from beneath the lobula midband (arrowed). (e). Enlarged view of the tongue. The boxed area is shown further enlarged, lower left. Notably, there are fewer axons representing the midband at this level than there are in layer 8–10 in the lobula, indicating that most midband neurons terminate in the lobula neuropil. (f, g) Golgi impregnated midband terminals in layers 10–12 showing vertically oriented collaterals extending from the midband (indicated by the double arrow). Scale bars (a, d, f, g) 50 μm; (b, c, e) 25 μm

4 | DISCUSSION

4.1 | Comparison of the stomatopod lobula with those of other pancrustaceans

Descriptions of the eumalacostracan lobula show it organized into columns and layers as it is in insects. But the crustacean lobula is generally denser, one major difference being that each of its columns represents one visual sampling unit whereas in most insects the lobula columns are spaced one to every six or nine sampling units (Strausfeld & Nässel, 1981; Sztarker et al., 2005; Harzsch & Hansson, 2008; Bengochea & Beron de Astrada, 2014). The stomatopod lobula also has a much greater depth of neuropil relative to lobulas in other studied eumalacostracans, or insects, and its volume clearly accommodates a much denser mass of neurons and their processes. While some of its columnar output neurons

ID: jwaa3b2server Time: 18:23 I Path: //chenas03.cadmus.com/Cenpro/ApplicationFiles/Journals/Wiley/CNE#/Vol00000/180008/Comp/APPFile/JW-CNE#180008

J_ID: Customer A_ID: CNE24398 Cadmus Art: CNE24398 Ed. Ref. No.: JCN-17-0275.R1 Date: 3-February-18 Stage: Page: 13

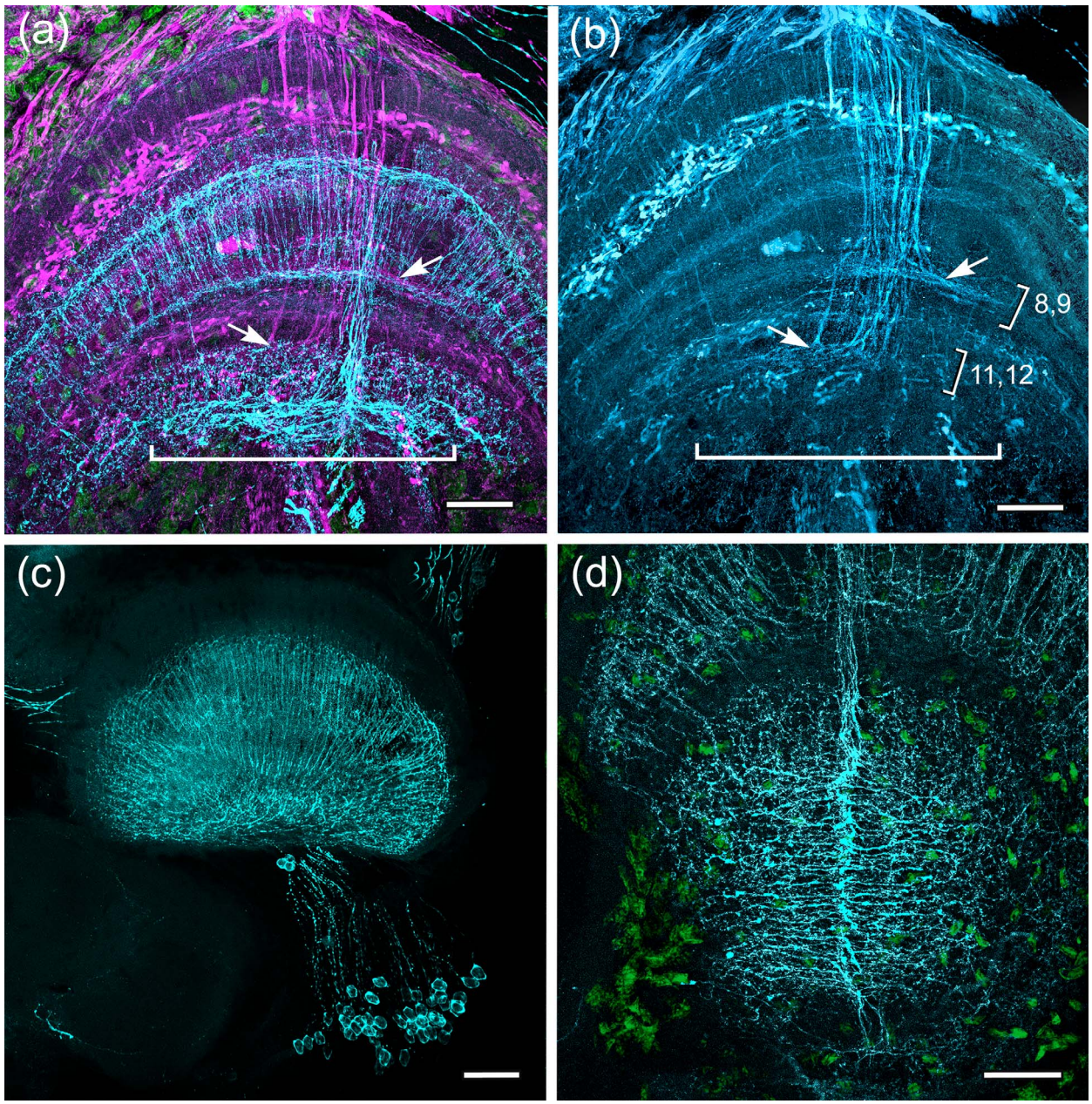

COLOR IN ONLINE AND PRINT

FIGURE 9 TH and GAD indicators of midband representation. Anti-TH immunostaining resolves at least three systems of TH-immunoreactive neurons associated with the midband's representation in the lobula. Notably all three systems are centered on the midband but extend their processes laterally so as to intersect retinotopic columns representing the upper and lower hemispheres. (a) Dual labeling with antibodies against GAD (magenta) and TH (cyan). Arrows indicate levels of collateral branches from GAD-positive terminals extending from the midband trajectory. These are shown just for the GAD-immunoreactive image in panel (b). As shown in Bodian stained material (Figure 7c), there are two levels at which MMP transmedullary neurons extend lateral branches: at layers 8/9 (outer arrow) and layers 11, 12 (inner arrow). (c). Origin of TH-positive local interneurons extending through layers 11–13 (panel a). (d) TH-positive local interneurons processes at layers 13 provide the deepest systems of lateral processes, the extents of which are indicated by the brackets in panels a, b (in panel d, the midband is shown extending vertically. In life, it is oriented horizontally and its lateral processes extend across retinotopic columns serving ommatidia that view a strip of the visual scene about 10° above and below the midband). Scale bars: 50 μm

have large axons and dendrites (Figure 5a) most have small diameter axons and both large and small neurons have narrow dendritic fields extending across immediately adjacent retinotopic columns.

The stomatopod lobula is also remarkable in possessing many planar networks of local interneurons arranged at the levels of collaterals extending from its columnar elements. Unlike the insect lobula, where there are few local interneurons, the stomatopod lobula is elaborately organized into a series of networks that suggest high-level computations. In terms of its neuroarchitecture, the lobula is less like its insect counterpart and more like the medulla that supplies its afferents. How elaborate these arrangements are will be discussed in a subsequent paper. Here, we show that some representations of the midband are wholly distinct

J_ID: Customer A_ID: CNE24398 Cadmus Art: CNE24398 Ed. Ref. No.: JCN-17-0275.R1 Date: 3-February-18 Stage: Page: 14

from other arrangements in the lobula's hemispheral parts (as is indeed the case in the medulla) but that there is also cross-talk between all three eye regions at specific depths: in the lower third of the medulla, constrained to an area representing about 10° of view each side of the midband (Figure 2e) and a far more extensive lateral representation in the lower third of the lobula (Figures 9d, 10). That is, most of the integration between eye regions and between color, polarization, and luminance occurs in the lobula. The small amount of integration that the medulla seems to allow is again the subject of a future article.

To summarize: there is both segregation of information from defined eye regions and representations of these into areas deep in the lobula, bearing in mind that there are also areas or layers along the way in the lobula that appear to allow integration of these parallel streams of information. MMP supplies devoted relay neurons, the axons of which define a narrow curtain-like array stretching across both the medulla's and lobula's horizontal extent (Figure 10). In the lobula information carried by these neurons extends at right angles along the vertical row of retinotopic columns relaying from the hemispheres. It is this system of collaterals that is pivotal to any discussion of integration amongst the chromatic, achromatic and polarization pathways. F10

4.2 | The stomatopod midband pathway and its possible roles in integrating chromatic/polarization information

Clearly, the organization of the midband in the lobula reveals the presence of a unique set of circuits for visual channel mixing, unsurprisingly not seen in any other pancrustacean as their retinal complexity and information channel-set is nowhere near as complex as in the stomatopod. Such an arrangement would suggest that as the eye scans a scene, its midband samples the spectral, UV-l-pol and c-pol composition and integrates this information with luminance and L-pol light information carried by channels from the upper and lower retinal hemispheres. This arrangement is wholly distinct from that in insects, which are renowned for their color vision. In the hymenopteran for example, chromatic and achromatic information is segregated at different levels in the lobula, the latter in a deep layer equivalent to the fly's lobula plate, before

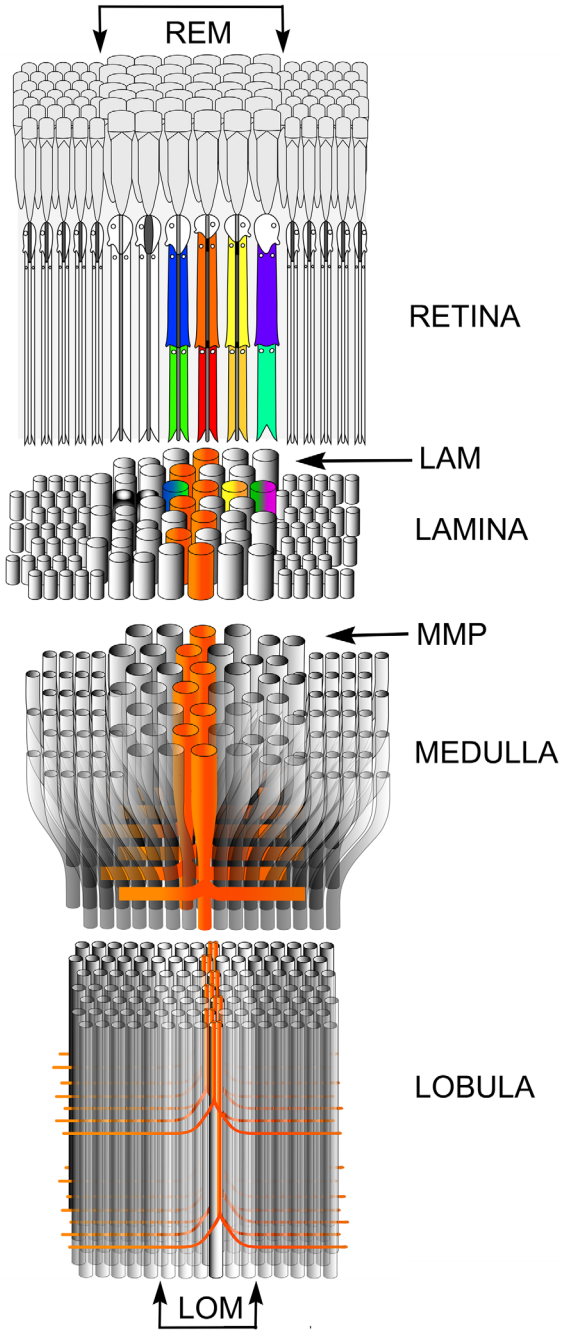

FIGURE 10 Schematic diagram showing midband representation through the optic lobe neuropils. In any vertical row of ommatidia extending across the eye, there are six midband ommatidia (retinal midband, REM). Counting from the top down, rows 1–4 of the midband contain eight photoreceptors. The distally placed R8 cells are UV sensitive. The underlying seven cells are sensitive to a different part of the human visible (400–700 nm) spectrum (indicated approximately by colors). The two rows of ommatidia beneath this, rows 5 and 6, contain circularly polarized light-sensitive photoreceptors capped by a UV-sensitive eighth photoreceptor that is also sensitive to linear polarization. Achromatic, linear-polarization-sensitive photoreceptors also exist in the main rhabdom (seven cells) of the ommatidia of the upper and lower hemispheres, flanking each side of the midband. The R8 cells here are UV sensitive but polarization insensitive. This retinal organization is precisely mapped into the optic cartridges of the lamina by the terminals of photoreceptor neurons (see Thoen et al., 2017b). Each cartridge represents the two chromatic channels of the ommatidium that supplies it. Here for clarity, only the orange-red channels of row 4 distal main rhabdom are shown extending through a small part of the succession of optic neuropils. At two levels, the midband forms an equatorial swelling (LAM in the lamina and MMP in the outer medulla) or a specialized zone (in the inner part of the medulla and through the lobula). Neurons relaying the midband representation from the MMP provide systems of lateral collaterals in the inner layers of the medulla. These extend through a limited number of columns representing the upper and lower hemispheres. Axons from the medulla midband columns reach the lobula where they define a discrete equatorial zone of retinotopic columns (lobula midband, LOM), in which they provide at least two levels of broad terminals: these branches extend further than the collaterals in the medulla

COLOR IN ONLINE AND PRINT

J_ID: Customer A_ID: CNE24398 Cadmus Art: CNE24398 Ed. Ref. No.: JCN-17-0275.R1 Date: 3-February-18 Stage: Page: 15

they project separately to specific centers in the midbrain (Paulk et al., 2008).

In the stomatopod, broad interaction amongst information channels appears to mainly occur deep in the lobula. The absence of any evidence that stratified processes interact with through-going axons of midband neurons suggests that midband channels comprise the most direct pathway from the retina to deep levels of the lobula, possibly involving few if any combinatorial interactions en route. Such a direct path from the midband to the deep lobula implies that information may be made available by the midband to lateral achromatic channels before they participate in high level reconstructions of the identical visual scene. But this view is complicated by evidence showing that already in the medulla, midband neurons have processes that extend laterally (Figure 10). And at that level there are numerous strata of local interneurons that contribute to computational levels that, presumably, can provide higher level processing among channels from the midband and the hemispheres. Thus, at the deepest level of the lobula, outputs representing the eye hemispheres may already encode combinatorial information provided by achromatic and UV-pol channels that have also already received chromatic inputs in the medulla.

In truth, until we have a more exact and cell-by-cell description of what information channel is shared with each other, it will remain difficult to determine exactly how stomatopods view the world. That said, there are a number of hypotheses worth erecting at this stage to provide a substrate for future tests, both anatomically and with other electrophysiological and behavioral methods. For example, if connections amongst chromatic rows occur within the MMP, as its elaborate anatomy could suggest, then a system of four dichromatic comparisons would be plausible. Such a combinatorial arrangement was originally suggested when the system was first described by Marshall (1988) and subsequently in Marshall et al. (2007). As well as potentially allowing some form of chromatic analysis, each ommatidium-based dichromatic comparison could discount luminance flicker, an idea originally proposed, though not in the stomatopod context, for the evolution of color vision in all animals (Maximov 2000).

Another point to consider is that the midband may serve as a spectrometer and collect chromatic information as a set of 12 bins across the wavelength range from 300 to 720 nm. This serial color processing or pattern analysis hypothesis, which recently received behavioral support (Thoen, How, Chiou, & Marshall, 2014), does not exclude some comparison of chromatic channels but it does fit well with a scanning analysis of objects, as made necessary by the line-scan optics and indeed eye movements of stomatopods (Marshall & Land 1993, Land, Marshall, Brownless, & Cronin, 1990). Having discovered or detected where a colored object is within the visual scene, using acquisitioned or saccadic eye movements (Marshall, Land, & Cronin, 2014), a switch to scanning the object with a spectrophotometer-like linear array may fill in information about the nature of the object. It should be remembered that both luminance and all forms of polarization information are also acquired simultaneously, as all eye areas view the same narrow band in space (Marshall & Land 1993).

That the organization of the stomatopod's midband suggests several interpretations is further illustrated by the evidence that chromatic information processing in photoreceptors may come at the cost of reduced speed compared to achromatic information processing (Skorupski & Chittka, 2010). Might stomatopods have organized their chromatic and achromatic systems so that midband relays involve fewer synaptic stations than achromatic relays and thus compensate for tardy transduction? Combined with the stomatopods scanning eye movements (Land et al., 1990; Marshall et al., 2014) the segregated chromatic processing would allow for signals to be integrated simultaneously, albeit peculiarly deep in the system.

The proposed integration of chromatic and achromatic information at this late stage may also serve the purpose relating to color constancy (maintaining stable color perception under varying illumination). Unlike the dichromatic Maximov-mechanism suggested above that would only function in a system of dichromatic comparisons, the color processing system suggested in Thoen et al. (2014) and Zaidi, Marshall, Thoen, and Conway (2014), would still need a luminance or pan-chromatic input to permit illuminant-independent color analysis. The binned, possibly interval decoding type of color processing that this second hypothesis suggests would combine the color information provided by rows 1–4 of the midband with the achromatic information from hemispheres to accurately interpret the perceived color. That is, the broadband, achromatic photoreceptors in the hemispheres would provide intensity information and the channel-mixing in the lobula would provide the color constancy needed to ensure reliable color perception.

4.3 | Neural substrates for motion vision

The range of stomatopod eye movements, in particular the frequently used scanning eye movements, makes it hard to envisage how they identify moving objects and locate them in the world around them. This is especially so as actual stabilization or optokinetic-style eye movements that allow most animals to fix their position in the world are relatively rare in stomatopods (Cronin, Marshall, & Land, 1991).

Stomatopods are well known for their prey-capture abilities using a very rapid ballistic strike that must be coordinated by some sort of object tracking system (Caldwell & Dingle 1976). It is not clear which circuits in the stomatopod optic lobes would be suitable for detecting such local motion of potential prey, as seen in the achromatic frontolateral eyes of salticid spiders (Zurek, Taylor, Evans, & Nelson, 2010). Small-field columnar neurons in the dipteran lobula have for example been identified that respond to local motion of contrasting objects or edges (O'Carroll, 1993; Nordström, Barnett, & O'Carroll, 2006; Okamura & Strausfeld, 2007), but further investigations of neuronal identities in the stomatopod optic lobes are needed to make predictions about their movement detection circuits. It is possible that the ommatidia outside the midband and the strip of midband space that the hemispheres examine (the peripheral regions of the eye) are tasked with moving object detection. When detecting a movement, a section of the eye, equivalent to an acute zone or fovea (including the midband and parts of the hemispheres), is placed on the object and in some cases may track it with smooth pursuit eye movements (Cronin, Nair, Doyle, & Caldwell, 1988; Cronin, Yan, & Bidle, 1992; Marshall et al., 2014).

J_ID: Customer A_ID: CNE24398 Cadmus Art: CNE24398 Ed. Ref. No.: JCN-17-0275.R1 Date: 3-February-18 Stage: Page: 16

To further complicate the discussion, stomatopods use independent eye movements when they are kept stationary at one location. It is not known, but suspected from casual observation, that one mode of eye movement and information input such as object tracking may be coordinated by one eye while another task such as object scanning is performed by the other. The eyes do occasionally appear coordinated in tracking (Cronin, Nair, Doyle, & Caldwell, 1988; Cronin et al., 1992, 1994) or assume a coordinated posture in an approximately horizontal orientation when the animal is moving forward through the water (How and Marshall—unpublished). Whether this is true eye synchrony or just both eyes responding the same way to an object or situation is also unknown (Cronin, Marshall, Quinn, & King, 1994).

Other circuits could supply information about visual flow, as in flying insects, when they move fast over the substrate. It is during swimming and fast walking that the detection of visual flow fields may be advantageous. If stomatopods employ these parameters for motion balance then neurons analogous to those computing wide-field directional motion in the lobula plate of insects should be distributed across areas of the stomatopod's retinotopic mosaic. However, only diminutive lobula plate-like neuropils have been identified in crustaceans, including stomatopods (Strausfeld 2005; Sztarker et al., 2005). It is well known that some classes of insects employ visual flow detection to maintain visual balance during flight and that the computation of visual flow depends on a distinct subset of small neurons called bushy T-cells (Douglass & Strausfeld, 1995; Strausfeld & Lee, 1991). These provide local directional motion information across 3–4 adjacent visual sampling units. Information is sent by them to large tangential neurons in the tectum-like "lobula plate" that integrate inputs from bushy T-cells and relay information about global visual motion to flight motor neuron circuits (Hausen & Egelhaaf, 1989; Krapp, Hengstenberg, & Egelhaaf, 2001; Joesch, Schnell, Raghu, Reiff, & Borst, 2010; Borst, Haag, & Reiff, 2010; Maisak et al., 2013).

Highly maneuverable insects, which include Coleoptera and Lepidoptera, have lobula plates characterized by wide-field tangential neuron dendrites (Buschbeck & Strausfeld, 1996). The only crustacean known to have a tectum-like neuropil comparably equipped is the littoral isopod *Ligia occidentalis* (Strausfeld, 1998; Sinakevitch, Douglass, Scholtz, Loesel, & Strausfeld, 2003). In this species, the inputs to its lobula plate originate from the medulla and they are not morphologically comparable to bushy T-cells of insects. In other eumalacostracans, the diminutive satellite neuropil claimed as homologous cannot be comparable to a functional lobula plate. Its size precludes it from subtending the retinal field and there are no small-field bushy T-cells supplying it as they do to the insect lobula plate, despite recent claims (Bengochea, Beron de Astrada, Tomsic, & Sztarker, 2017). It is significant that bushy T-cells are absent in insects that are not accomplished fliers.

Although stomatopods rarely swim, when they do they are adept at it and they are astonishingly fast over-substrate movers either scuttling or swimming low, making them hard to catch. If they possess either tangential flow-field neurons or object spotting neurons, as their accuracy in prey-strike suggests, only the medulla and lobula possess systems functionally analogous to those of the lobula plate. At deep layers of the stomatopod medulla there are tangential neurons with wide dendritic fields extending vertically across the retinotopic mosaic, and looming detecting wide-field neurons have been identified at this level in the insect medulla (Wicklein & Strausfeld, 2000). In stomatopods, unlike insects, the largest and most numerous tangential neurons occur at several depths of the lobula, many of which extend their dendrites across a large part of it. Although we are still ignorant regarding their response properties, the location, size, and dendritic orientations of these neurons suggest that they are the most likely candidates for a role in detecting large-field visual motion like flow-fields or may be involved in the tracking of small objects.

ACKNOWLEDGMENTS

This work was supported by grants to JM from the U.S. Air Force Research Laboratory (FA8651-13-1-0001, FA8651-17-P-0121), a U. S. Air Force Research Laboratory STTR/SBIR grant F17A-021-0188 to NJS, grants to JM from the Asian Office of Aerospace Research and Development (FA23861314134) and the Australian Research Council (FL140100197), and a doctoral fellowship (2013) to HHT from the Lizard Island Research Foundation, a facility of the Australian Museum. The Zeiss LSM 710 inverted point-scanning confocal was funded by an ARC lief grant no. LE130100078. We are grateful to the QBI imaging facility for its support and thank Roy Caldwell for the image for Figure 1a.

CONFLICT OF INTEREST

The authors have no conflicts of interest.

ORCID

Hanne Halkinrud Thoen http://orcid.org/0000-0001-8695-9578
Nicholas James Strausfeld http://orcid.org/0000-0002-1115-1774

REFERENCES

Bengochea, M., & Beron de Astrada, M. (2014). Organization of columnar inputs in the third optic ganglion of a highly visual crab. *Journal of Physiology Paris*, *108*(2–3), 61–70. doi.org/10.1016/j.jphysparis.2014.05.005

Bengochea, M., Beron de Astrada, M., Tomsic, D., & Sztarker, J. (2017). A crustacean lobula plate: Morphology, connections, and retinotopic organization. *The Journal of Comparative Neurology*, *526*(1), 109–119. https://doi.org/10.1002/cne.24322

Bodian, D. (1936). A new method for staining nerve fibers and nerve endings in mounted paraffin sections. *The Anatomical Record*, *65*(1), 89–97. https://doi.org/10.1002/ar.1090650110

Borst, A., Haag, J., & Reiff, D. F. (2010). Fly motion vision. *Annual Review of Neuroscience*, *33*, 49–70. doi.org/10.1146/annurev-neuro-060909-153155

Buschbeck, E. K., & Strausfeld, N. J. (1996). Visual motion-detection in flies: Small-field retinotopic elements responding to motion are evolutionarily conserved across taxa. *Journal of Neuroscience*, *16*, 1563–1578.

Caldwell, R. L., & Dingle, H. (1976). Stomatopods. *Scientific American*, *234*(1), 80–89.

Chiou, T.-H., Kleinlogel, S., Cronin, T. W., Caldwell, R., Loeffler, B., Siddiqi, A., & Marshall, N. J. (2008). Circular polarization vision in a

J_ID: Customer A_ID: CNE24398 Cadmus Art: CNE24398 Ed. Ref. No.: JCN-17-0275.R1 Date: 3-February-18 Stage: Page: 17

stomatopod crustacean. *Current Biology*, *18*(6), 429–434. doi.org/10.1016/j.cub.2008.02.066

Cronin, T. W., & Marshall, N. J. (1989). A retina with at least ten spectral types of photoreceptors in a mantis shrimp. *Nature*, *339*(6220), 137–140. https://doi.org/10.1038/339137a0

Cronin, T. W., Marshall, N. J., & Caldwell, R. L. (1993). Photoreceptor spectral diversity in the retinas of squilloid and lysiosquilloid stomatopod crustaceans. *Journal of Comparative Physiology A*, *172*(3), 339–350. doi.org/10.1007/BF00216616

Cronin, T. W., Marshall, N. J., & Land, M. F. J (1991). Optokinesis in gonodactyloid mantis shrimps (Crustacea; Stomatopoda; Gonodactylidae). *Journal of Comparative Physiology A*, *168*, 233. doi.org/10.1007/BF00218415

Cronin, T. W., Marshall, N. J., & Land, M. (1994). The unique visual system of the mantis shrimp. *American Scientist*, *82*, 356–365.

Cronin, T. W., Marshall, N. J., Quinn, C. A., & King, C. A. (1994). Ultraviolet photoreception in mantis shrimp. *Vision Research*, *34*(11), 1443–1452. doi.org/10.1016/0042–6989(94)90145-7

Cronin, T. W., Nair, J. N., Doyle, R. D., & Caldwell, R. L. (1988). Ocular tracking of rapidly moving visual targets by stomatopod crustaceans. *Journal of Experimental Biology*, *138*, 155–179.

Cronin, T. W., Yan, H. Y., & Bidle, K. D. (1992). Regional specialisation for control of ocular movements in the compound eyes of a stomatopod crustacean. *Journal of Experimental Biology*, *171*, 373–393.

Derby, C. D., Fortier, J. K., Harrison, P. J. H., & Cate, H. S. (2003). Peripheral and central antennular pathway of the Caribbean stomatopod crustacean Neogonodactylus oerstedii. *Arthropod Structure & Development*, *32*, 175–188. https://doi.org/ 10.1016 S1467-8039(03)00048-3

Douglass, J. K., & Strausfeld, N. J. (1995). Visual motion detection circuits in flies—peripheral motion computation by identified smallfield retinotopic neurons. *Journal of Neuroscience*, *15*, 5596–5611.

Ehmer, B., & Gronenberg, W. (2002). Segregation of visual input to the mushroom bodies in the honeybee (*Apis mellifera*). *The Journal of Comparative Neurology*, *451*(4), 362–373. https://doi.org/10.1002/cne.10355

Harzsch, S., & Hansson, B. S. (2008). Brain architecture in the terrestrial hermit crab Coenobita clypeatus (Anomura, Coenobitidae), a crustacean with a good aerial sense of smell. *BMC Neuroscience*, *9*(1), 58. https://doi.org/10.1186/1471-2202-9-58

Hausen, K., & Egelhaaf, M. (1989). Neural mechanisms of visual course control in insects. In D. G. Stavenga & R. C. Hardie (Eds.) *Facets of vision* (pp. 391–424). Berlin: Springer. doi.org/10.1007/978-3-642–74082-4_18

Joesch, M., Schnell, B., Raghu, S. V., Reiff, D. F., & Borst, A. (2010). ON and OFF pathways in Drosophila motion vision. *Nature*, *468*, 300–304. https://doi.org/10.1038/nature09545

Klagges, B. R. E., Heimbeck, G., Godenschwege, T. A., Hofbauer, A., Pflugfelder, G. O., Reifegerste, R., . . . Buchner, E. (1996). Invertebrate synapsins: A single gene codes for several isoforms in Drosophila. *Journal of Neuroscience*, *16*(10), 3154–3165.

Kleinlogel, S., Marshall, N. J., Horwood, J. M., & Land, M. F. (2003). Neuroarchitecture of the color and polarization vision system of the stomatopod Haptosquilla. *The Journal of Comparative Neurology*, *467*(3), 326–342. https://doi.org/10.1002/cne.10922

Kleinlogel, S., & Marshall, N. J. (2005). Photoreceptor projection and termination pattern in the lamina of gonodactyloid stomatopods (mantis shrimp). *Cell and Tissue Research*, *321*(2), 273–284. doi.org/10.1007/s00441-005-1118-4

Krapp, H. G., Hengstenberg, R., & Egelhaaf, M. (2001). Binocular contributions to optic flow processing in the fly visual system. *Journal of Neurophysiology*, *85*(2), 724–734.

Land, M. F., Marshall, N. J., Brownless, D., & Cronin, T. W. (1990). The eye-movements of the mantis shrimp Odontodactylus Scyllarus (Crustacea, Stomatopoda). *Journal of Comparative Physiology A*, *167*(2), 155–166. doi.org/10.1007/BF00188107

Lebhart, F., & Desplan, C. (2017). Retinal perception and ecological significance of color vision in insects. *Current Opinion in Insect Science*, *24*, 75–83. doi.org/10.1016/j.cois.2017.09.007

Li, Y., & Strausfeld, N. J. (1997). Morphology and sensory modality of mushroom body extrinsic neurons in the brain of the cockroach, Periplaneta americana. *Journal of Comparative Neurology*, *387*(4), 631–650. doi.org/10.1002/(SICI)1096–9861(19971103)387:4 < 631::AID-CNE9 > 3.0.CO;2–3

Lin, T.-Y., Luo, J., Shinomiya, K., Ting, C.-Y., Lu, Z., Meinertzhagen, I. A., & Lee, C.-H. (2016). Mapping chromatic pathways in the Drosophila visual system. *Journal of Comparative Neurology*, *524*, 213–227. https://doi.org/10.1002/cne.23857

Maisak, M. S., Haag, J., Ammer, G., Serbe, E., Meier, M., Leonhardt, A., & Nern, A. (2013). A directional tuning map of Drosophila elementary motion detectors. *Nature*, *500*(7461), 212–216. https://doi.org/10.1038/nature12320

Marshall, N. J. (1988). A unique colour and polarization vision system in mantis shrimps. *Nature*, *333*(6173), 557–560. https://doi.org/10.1038/333557a0.

Marshall, N. J., Cronin, T. W., & Kleinlogel, S. (2007). Stomatopod eye structure and function: a review. *Arthropod Structure & Development*, *36*(4), 420–448. doi.org/10.1016/j.asd.2007.01.006

Marshall, N. J., & Land, M. F. (1993). Some optical-features of the eyes of Stomatopods I. Eye shape, optical axes and resolution. *Journal of Comparative Physiology A-Sensory Neural and Behavioral Physiology*, *173*(5), 565–582. doi.org/10.1007/BF00197766

Marshall, N. J., Land, M. F., & Cronin, T. W. (2014). Shrimps that pay attention: Saccadic eye movements in stomatopod crustaceans. *Philosophical Transactions Royal Society London B: Biological Sciences*, *369*(1636), 20130042. doi.org/10.1098/rstb.2013.0042

Marshall, J., Kent, J., & Cronin, T. (1999). Visual adaptations in crustaceans: spectral sensitivity in diverse habitats. In S. Archer, M. B. Djamgoz, E. Loew, J.C. Partridge, & S. Vallerga (Eds.) *Adaptive mechanisms in the ecology of vision* (pp. 285–327). Dordrecht: Springer. doi.org/10.1007/978-94-017–0619-3_10

Marshall, N. J., & Oberwinkler, J. (1999). Ultraviolet vision: The colourful world of the mantis shrimp. *Nature*, *401*(6756), 873–875. https://doi.org/10.1038/44751

Maximov, V. V. (2000). Environmental factors which may have led to the appearance of colour vision. *Philosophical Transactions of the Royal Society of London Series B-Biological Sciences*, *355*(1401), 1239–1242. https://doi.org/10.1098/rstb.2000.0675

Mu, L., Ito, K., Bacon, J. P., & Strausfeld, N. J. (2012). Optic glomeruli and their inputs in Drosophila share an organizational ground pattern with the antennal lobes. *The Journal of Neuroscience*, *32*(18), 6061–6071. doi.org/10.1523/JNEUROSCI.0221-12.2012

Nordström, K., Barnett, P. D., & O'Carroll, D. C. (2006). Insect detection of small targets moving in visual clutter. *PLoS Biology*, *4*, e54. doi.org/10.1371/journal.pbio.0040054

O'Carroll, D. (1993). Feature-detecting neurons in dragonflies. *Nature*, *362*(6420), 541–543. https://doi.org/10.1038/362541a0

Okamura, J.-Y., & Strausfeld, N. J. (2007). Visual system of calliphorid flies: Motion- and orientation-sensitive visual interneurons supplying dorsal optic glomeruli. *The Journal of Comparative Neurology*, *500*, 189–208. https://doi.org/10.1002/cne.21195

Paulk, A. C., Phillips-Portillo, J., Dacks, A. M., Fellous, J. M., & Gronenberg, W. (2008). The processing of color, motion, and stimulus timing are

anatomically segregated in the bumblebee brain. *The Journal of Neuroscience*, *28*(25), 6319–6332. doi.org/10.1523/JNEUROSCI.1196-08.2008

Rister, J., & Desplan, C. (2011). The retinal mosaics of opsin expression in invertebrates and vertebrates. *Developmental Neurobiology*, *71*, 1212–1226. https://doi.org/10.1002/dneu.20905

Roberts, N. W., Chiou, T.-H., Marshall, N. J., & Cronin, T. W. (2009). A biological quarter-wave retarder with excellent achromaticity in the visible wavelength region. *Nature Photonics*, *3*(11), 641–644. https://doi.org/10.1038/nphoton.2009.189

Schindelin, J., Arganda-Carreras, I., Frise, E., Kaynig, V., Longair, M., Pietzsch, T., ... Cardona, A. (2012). Fiji: An open-source platform for biological-image analysis. *Nature Methods*, *9*(7), 676–682. https://doi.org/10.1038/nmeth.2019

Sinakevitch, I., Douglass, J. K., Scholtz, G., Loesel, R., & Strausfeld, N. J. (2003). Conserved and convergent organization in the optic lobes of insects and isopods, with reference to other crustacean taxa. *The Journal of Comparative Neurology*, *467*(2), 150–172. https://doi.org/10.1002/cne.10925

Skorupski, P., & Chittka, L. (2010). Differences in photoreceptor processing speed for chromatic and achromatic vision in the bumblebee, Bombus terrestris. *The Journal of Neuroscience*, *30*(11), 3896–3903. doi.org/10.1523/JNEUROSCI.5700-09.2010

Strausfeld, N. J. (1998). Crustacean - Insect relationships: The use of brain characters to derive phylogeny amongst segmented invertebrates. *Brain, Behavior and Evolution*, *52*(4–5), 186–206. doi.org/10.1159/000006563

Strausfeld, N. J. (2005). The evolution of crustacean and insect optic lobes and the origins of chiasmata. *Arthropod Structure and Development*, *34*(3), 235–256. doi.org/10.1016/j.asd.2005.04.001

Strausfeld, N. J., & Lee, J. K. (1991). Neuronal basis for parallel visual processing in the fly. *Visual Neuroscience*, *7*, 13–33. https://doi.org/10.1017/S0952523800010919

Strausfeld, N. J., & Nässel, D. R. (1981). Neuroarchitectures serving compound eyes of Crustacea and insects. In H. Atrum (ed.) *Comparative physiology and evolution of vision in invertebrates B invertebrate visual centres and behavior I. Vol VII/6B. Handbook of sensory physiology*. Berlin: Springer.

Strausfeld, N. J., Sinakevitch, I., & Okamura, J. Y. (2007). Organization of local interneurons in optic glomeruli of the dipterous visual system and comparisons with the antennal lobes. *Developmental Neurobiology*, *67*(10), 1267–1288. https://doi.org/10.1002/dneu.20396

Sullivan, J. M., & Beltz, B. S. (2004). Evolutionary changes in the olfactory projection neuron pathways of eumalacostracan crustaceans. *The Journal of Comparative Neurology*, *470*(1), 25–38. https://doi.org/10.1002/cne.11026

Sztarker, J., Strausfeld, N. J., & Tomsic, D. (2005). Organization of optic lobes that support motion detection in a semiterrestrial crab. *The Journal of Comparative Neurology*, *493*(3), 396–411. https://doi.org/10.1002/cne.20755

Templin, R. M., How, M. J., Roberts, N. W., Chiou, T.-H., & Marshall, J. (2017). Circularly polarized light detection in stomatopod crustaceans: A comparison of photoreceptors and possible function in six species. *The Journal of Experimental Biology*, *220*(18), 3222–3230. https://doi.org/10.1242/jeb.162941

Thoen, H. H., How, M. J., Chiou, T.-H., & Marshall, N. J. (2014). A different form of color vision in mantis shrimp. *Science (New York, N.Y.)*, *343*(6169), 411–413. https://doi.org/10.1126/science.1245824

Thoen, H. H., Chiou, T.-H., & Marshall, N. J. (2017a). Intracellular recordings of spectral sensitivities in stomatopods: A comparison across species. *Integrative and Comparative Biology*, *57*(5), 1117–1129. https://doi.org/10.1093/icb/icx111

Thoen, H. H., Strausfeld, N. J., & Marshall, J. (2017b). Neural organization of afferent pathways from the stomatopod compound eye. *The Journal of Comparative Neurology*, *525*, 3010–3030. https://doi.org/10.1002/cne.24256

Wicklein, M., & Strausfeld, N. J. (2000). Organization and significance of neurons that detect change of visual depth in the hawk moth *Manduca sexta*. *The Journal of Comparative Neurology*, *424*, 356–376. https://doi.org/10.1002/1096-9861(20000821)424:2<356::AID-CNE12>3.0.CO;2-T

Wolff, G., & Strausfeld, N. J. (2016). The insect brain: A commentated primer. In A. Schmidt-Rhaesa, S. Harzsch, & G. Purschke (eds.) *Structure and evolution of invertebrate nervous systems* (pp. 957–639). Oxford: Oxford University Press.

Wolff, G., Thoen, H. H., Marshall, N. J., Sayre, M. E., & Strausfeld, N. J. (2017). An insect-like mushroom body in a crustacean brain. *eLife*, *6*, e29889. https://doi.org/10.7554/eLife.29889

Zaidi, Q., Marshall, N. J., Thoen, H. H., & Conway, B. R. (2014). Evolution of neural computations: Mantis shrimp and human color decoding. *i-Perception*, *5*(6), 492–496. doi.org/10.1068/i0662sas

Zurek, D. B., Taylor, A. J., Evans, C. S., & Nelson, X. J. (2010). The role of the anterior lateral eyes in the vision-based behaviour of jumping spiders. *Journal of Experimental Biology*, *213*, 2372–2378. https://doi.org/10.1242/jeb.042382

How to cite this article: Thoen HH, Sayre ME, Marshall J, Strausfeld NJ. Representation of the stomatopod's retinal mid-band in the optic lobes: Putative neural substrates for integrating chromatic, achromatic and polarization information. *J Comp Neurol*. 2018;00:1–18. https://doi.org/10.1002/cne.24398

SGML and CITI Use Only
DO NOT PRINT

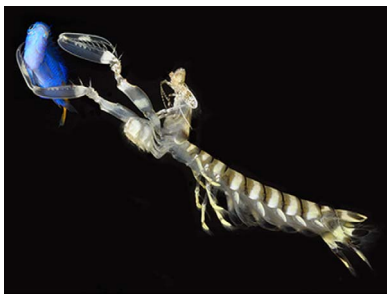

The stomatopod (mantis shrimp), *Lysiosquillina maculata* in the act of spearing a damselfish. The raptorial strike is 40 times faster than that of its land-based insect namesake, the praying mantis. The visual system mediating the stomatopod's predatory behaviors originated over 400 million years ago. This paper examines the neuronal relay system housed within the eyestalk that allows the coordination of these raptorial movements. Neuropils beneath the eye coordinate information from 20 or more parallel retinal channels including 12 color sensitivities, six polarization channels, and spatial information from thousands of achromatic receptors. This article is the second of a series discovering how this barrage of sensory information is reduced to supply circuits coordinating such complex behavior. Image courtesy of Professor Roy Caldwell, University of California, San Diego.